Supporting Information

Oxidative carbon backbone rearrangement in rishirilide biosynthesis

Olga Tsypik[†], Roman Makitrynskyy[†], Britta Frensch[‡], David L. Zechel[§], Thomas Paululat[‡‡], Robin Teufel[‡,*], and Andreas Bechthold[†,*]

[†] Department of Pharmaceutical Biology and Biotechnology, Institute of Pharmaceutical Sciences, Albert-Ludwigs-Universität Freiburg, Stefan-Meier-Strasse 19, 79104, Freiburg, Germany; [‡] Faculty of Biology, Schänzlestr. 1, 79104, Freiburg, Germany. [§] Department of Chemistry, Queen's University, 90 Bader Lane, Kingston, K7L 3N6 Ontario, Canada; [‡‡] Organic Chemistry, University of Siegen, Adolf-Reichwein-Str. 2, 57068 Siegen, Germany.

*Correspondence: robin.teufel@zbsa.uni-freiburg.de & andreas.bechthold@pharmazie.uni-freiburg.de

Table of Contents

A. Bacterial strains culture conditions.

Bacterial strains and plasmids used in this work are listed in TableS1. *Escherichia coli* was grown at 37 °C in LB medium supplemented with the respective antibiotic if needed. *Streptomyces bottropensis* wild type and mutants were grown at 28 °C in liquid TSB medium. MS agar was used to grow and collect spores from *S. bottropensis*, as well as for intergeneric conjugation with *E. coli*.[1] For production of rishirilide and its intermediates, MYM medium supplemented with 0.25 % valine (MYM-v) was used. MYM consists of (per liter of deionized water): malt extract – 10 g, yeast extract – 4 g, maltose – 4 g, 2 ml R2YE trace elements solution, pH 7.2.

B. TableS1. Bacterial strains and plasmids used in this work.

Strain / Plasmid	**Characteristics**	**Source / Reference**
E. coli strains		
XL1Blue	general cloning host	Agilent
ET12567 (pUZ8002)	host used for *E.coli-Streptomyces* intergeneric conjugation, methylation deficient	2
BL21 (DE3) Star™	host for protein production	Thermo Fisher Scientific
BW25113 (pIJ790)	host for recombineering experiments	2
Streptomyces strains		
S. bottropensis	wild type strain, producer of rishirilide A, B and D	3
S. bottropensis rslO5::Sp	mutant with in frame replacement of *rslO5* with spectinomycin resistance cassette	This work
S. bottropensis ΔrslO8	*rslO8* in-frame deletion mutant	This work
S. bottropensis ΔrslO9	*rslO9* in-frame deletion mutant	This work
Plasmids		
pET28a(+)	cloning vector for His-tagged protein production in *E. coli*, kanamycin resistance	Novagen
pET28a-rslO5	pET28a derived plasmid for production of His-tagged RslO5	This work
pET28a-rslO8	pET28a derived plasmid for production of His-tagged RslO8	This work
pET28a-rslO9	pET28a derived plasmid for production of His-tagged RslO9	This work
pBluescript SK(-)	vector for routine cloning	Addgene
pBlueScript-O8	pBlueScript carrying rslO8 with 3-kb flanks	This work
pBlueScript-O9	pBlueScript carrying rslO9 with 3-kb flanks	This work
pBlueScript-O8::Am	pBlueScript carrying rslO8 replaced by apramycin cassette	This work
pBlueScript-O9::Am	pBlueScript carrying rslO9 replaced by apramycin cassette	This work
pLeere	apramycin cassette with loxP-sites for gene replacement	4
pKGLP2	suicide vector for gene replacement	5

pKGLP2-O8::Am	*rslO8* knockout construct	This work
pKGLP2-O9::Am	*rslO9* knockout construct	This work

C. Table S2. List of primers

Primer name	**Sequence**	**Purpose**
rslO8-f	CGGTGGACAGCTCCTGCAC	*rslO8* gene deletion
rslO8-r	CGGACGCGTACACCGAGAC	
rslO9-f	CTGCCATTGCGGATCCTTTC	*rslO9* gene deletion
rslO9-r	CTGCCATTGCGGATCCTTTC	
Sp-rslO5-f	GGCCTGTTCGGCTCGACCCCGTTCGGTGGCCTC ACCCTGGCTAGCGGAGCGTAGCGACCGAGTG	spectinomycin cassette for *rslO5* replacement
Sp-rslO5-r	GTGCTGGGCGGCGCGGGTACGTGGGGCGGACT TCGGTCAGCTAGCGGCTATTTAACGACCCTGC	
Am-rslO8-f	CGCGAAGCCCACTTCCCTCACCGCACCGCGAGG TTCCCATGGATATCTCTAGATACCG	apramycin cassette for *rslO8* replacement
Am-rslO8-r	TCGCGCTCTCTGGGTCATGGTGACGGGCTCCCG CGGATCAAACAAAAGCTGGAGCTC	
Am-rslO9-f	ACCCGCGCCCGCGCCCGCGCCCGCGCCCGACG AAACCGTGGATATCTCTAGATACCG	apramycin cassette for *rslO9* replacement
Am-rslO9-r	TGACGTTCGGGGAGGTGCGGGATGCCCTGCGG GCTGTTCAAACAAAAGCTGGAGCTC	
rslO5-NdeI-f	AATTAACATATGAGCGGCCTGTTCGGCTC	RslO5-His production
rslO5-XhoI-r	AACTCGAGGCCCGCGGTGCCC	
rslO8-NdeI-F	CGCGCATATGCGACTGATCAGCTATGACGA	RslO8-His production
rslO8-HindIII-r	TATCAAGCTTTCAGGGGACGAGGACGACAC	
rslO9-NdeI-F	AAACATATGACCCAGAGAGCGCGAC	RslO9-His production
rslO9-HindIII-r	ATAAAGCTT TCAGTGCGCGGGCCGGTGCA	
O5-H172N-F	AACGGCGCCAACGGCT	site directed mutagenesis of RslO5
O5-H172N-R	GATCTCGACGCCGT	
O5-N175H-F	CACGGCTATCTGCTGCAC	
O5-N175H-R	GGCGCCGTGGATCTC	
O5-Y177F-F	TTCCTGCTGCACCAGTTCC	
O5-Y177F-R	GCCGTTGGCGCCGTG	

D. Construction of gene deletion mutants

All mutants were constructed using λ-red mediated recombination technology.[2] To inactivate *rslO8* and *rslO9*, the suicide plasmids pKGLP2-O8::Am and pKGLP2-O9::Am were constructed. Initially, a DNA sequence with approximately 3 kb flanking region was amplified from cos4 using appropriate primers (Table S2). The PCR product was cloned into pBlueScript digested with EcoRV. The obtained plasmid was introduced into BW25113 (pIJ790) where replacement of the gene coding sequence by an apramycin resistance cassette was accomplished. Then, a DNA sequence carrying the replaced gene with its flanking regions was amplified with the same primers pair from newly obtained plasmid (for instance, pBlueScript-O8::Am) and ligated into blunt ends of pKGLP2 digested with EcoRV. The obtained plasmids

pKGLP2-O8::Am and pKGLP2-O9::Am were confirmed by restriction analysis and sequencing, and introduced into wild type *S. bottropensis* by intergeneric conjugation with *E. coli* ET12567 (pUZ8002) harboring the aforementioned constructs. The double cross-over mutants were screened for resistance to apramycin and sensitivity to hygromycin, and confirmed by PCR. To generate the marker-free mutants, apramycin resistance cassette was excised by Cre recombinase.[5] A mutant with *rslO5* deletion was constructed using the same procedure, except that the spectinomycin resistance gene was used and replacement was initially performed on the cosmid cos4-int::bla (where the integrase gene was replaced by ampicillin).

E. Strain fermentation and metabolite analysis.

Fresh or frozen spores of the wild type or mutant strains were inoculated into MYM-v and grown for five days with a rotary shaking at 180 rpm. After cultivation, the supernatant was extracted with the same volume of ethyl acetate, evaporated and dissolved in methanol. The methanol extract was directly used for LC-MS analysis on a Thermo Fisher LC/MSD TSQ Quantum Access Max machine. For the LC analysis, a Zorbax Eclipse Plus C18 column (1.8 mcm, 2.1 mm × 50 mm) from Agilent was used (mobile phase A: H_2O and mobile phase B: acetonitrile, both with 0.5% CH_3COOH). The solvents were delivered at 0.5 mL/min with the following gradient: 0 min 80% A, 0.5 min 80% A, 8 min 5% A, 9 min 5% A, 9.1 min 80% A, 11 min 80% A. The mass spectrometer was operated in negative ion ESI mode, with an ion-spray voltage of -2.5 kV, source temperature of 450 °C. The pressures of sheath and auxiliary gas (N_2) were set to 25 and 5 (arbitrary units) respectively. The ion transfer tube was heated up to 320 °C.

F. Isolation and purification of compounds.

For large scale production, 4 to 8 liters of MYM-v was inoculated from a seed culture which were grown in TSB medium for 24-36 hours. Compound **4** was purified from *S. bottropensis* rslO5::Sp. The cultures were centrifuged to remove biomass. The supernatant was decanted and adjusted to pH 4.0 with HCl, then exhaustively extracted with ethyl acetate. The organic phase was collected and evaporated. The extract was dissolved in 40% methanol and fractionated using solid phase extraction column [Oasis HLB 35cc (6g) LP Extraction Cartridge, Waters GmbH, Eschborn, Germany] with subsequent gradient elution with increasing concentrations of methanol. The fraction containing desired compounds was concentrated *in vacuo* and further purified by semi-preparative HPLC on an Agilent 1100 HPLC system with a DAD detector equipped with a Zorbax SB column (C18, 9.4×150 mm, 5 μm, Agilent Techonologies). The following elution gradient was used: 0 min 40% A, 8 min 0% A, 9 min 0% A, 10 min 40% A, 12 min 40% A (mobile phase A: H_2O with 0.5% CH_3COOH as a solvent modifier and mobile phase B: acetonitrile). The solvents were delivered at 2.5 mL/min.

For **4** purification the following elution gradient was used: 0 min 30% A, 1 min 30% A, 11 min 5% A, 12 min 5% A, 12.5 min 30% A, 14 min 30% A (mobile phase A: H_2O with 0.5% CH_3COOH as a solvent modifier and mobile phase B: acetonitrile).

Compounds **3** and **5** were purified from *S. bottropensis* Δ*rslO6* and *S. bottropensis* Δ*rslO9*, respectively. The supernatant from the culture was adjusted to pH 6.5 and extracted twice with the same amount of ethyl acetate. The resulting crude extract was dried and dissolved in 40%

methanol. Initially, compounds were separated on solid phase extraction column by gradient elution with increasing methanol concentrations. Fractions containing compound **3** and **5** were further purified by the semi-preparative HPLC as describes before with the following elution gradient: 0 min 40% A, 8 min 0% A, 9 min 0% A, 10 min 40% A, 12 min 40% A (mobile phase A: H_2O with 0.5% CH_3COOH as a solvent modifier and mobile phase B: acetonitrile). The solvents were delivered at 2.5 mL/min. **3** was evaporated under nitrogen flow.

G. Protein production and purification

All proteins used in this work were produced with N-terminal hexahistidine tag. The ORFs of *rslO5*, *rslO8* and *rslO9* were amplified with primers pair listed in Table S2 from genomic DNA of *S. bottropensis*. The PCR products were digested with NdeI and HindIII or in case of *rslO5* with NdeI and XhoI restriction enzymes, and ligated into respective sites of pET28a. After sequencing, the obtained plasmids pET28a-rslO5, pET28a-rslO8 and pET28a-rslO9 were transformed into *E. coli* BL21 (DE3) Star ™. One colony was grown for a seed culture in LB medium supplemented with 50 µg/ml kanamycin. The pre-culture was grown overnight then used to inoculate 1 L main culture (1% v/v), which was then grown at 37 °C until the OD_{600} reached 0.5. Protein production was induced with 0.1 mM IPTG, and culture was then allowed to grow at 18 °C for another 16-18h.

For RslO9 and RslO8 purification, the collected cell pellet was resuspended in a lysis buffer (50 mM TrisHCl, 500 mM NaCl, 10 mM imidazole, pH 7.5, supplemented with 1 mM PMSF and 1 µg/ml DNaseI), and cells were disrupted by two passes through French Press. The crude lysate was then centrifuged at +4 °C at 10000 rpm for 30 min and the protein was purified from a soluble fraction by affinity chromatography using Ni-NTA beads with elution buffer (50 mM TrisHCl, 500 mM NaCl, 200 mM imidazole, pH 7.0). The purity of the protein was analyzed by SDS-PAGE and protein concentration was determined by the Bradford assay. The storage buffers of the proteins contained 5 % glycerol.

RslO5 and its mutated versions were purified using 50 mM phosphate buffer (50 mM Na_2HPO_4, 500 mM NaCl, with 20 or 200 mM imidazole in lysis and elution buffer, respectively, pH 7.0). To produce RslO5 variants with mutations in putative active site, plasmids encoding single amino acid replacement were constructed. For this purpose, the entire plasmid pET28a-*rslO5* was amplified with the primers pair (see Table S2), where the forward primer introduced the mutation of interest. Then, the obtained PCR product was purified, phosphorylated with T4 polynucleotide kinase, then self-ligated using T4 DNA ligase. The desired mutation was confirmed by DNA sequencing.

Detailed analysis of the *rslO9* ORF together with BLAST searches revealed the presence of two putative translational start codons. In contrast to the (mis)annotated sequence of RslO9 (AHL46732.1), only the longer version of the protein carrying 31 additional amino acids (Figure S23) produced a soluble protein upon heterologous expression and thus this version was used to perform *in vitro* assays.

H. *In vitro* enzyme assays

***In vitro* assay of RslO5.** An assay mixture (100 µL) containing RslO5 (5 µM), compound **4** (100 µM), FMN (1 µM), NADPH (1 mM) and Tris buffer (pH 8.0, 50 mM) was incubated at

28 ̊C for 30 min. To terminate the reaction, 100 µl assay mixture was mixed with 500 µL of ethyl acetate/acetic acid (99:1), shaken for 10 min, then centrifuged to separate phases. The organic phase containing reaction product(s) was filtered with a PVDF 0.2 µm filter, evaporated, then dissolved in 60 µL of methanol. Five µL were injected for HPLC analysis to monitor reactions result with the method aforementioned in Section F. The control reactions were carried out under the same conditions with heat inactivated enzyme, by omitting FMN or NADPH, or by replacing NADPH with NADH (1 mM). *In vitro* assays with RslO5 active site variants were carried out with respective protein (2.5 µM) in the same way as described above.

In order to identify a true intermediate of the pathway from *S. bottropensis rslO5*::Sp, purified RslO5 was also incubated with 10 µL of crude extract (the methanol from the extract was first evaporated and re-dissolved in 5 µL of DMSO to prevent protein denaturation).

***In vitro* assay of RslO9**. Enzymatic reaction (100 µL) containing RslO9 (5 µM), compound **5** (100 µM), NADPH (1 mM) and Tris buffer (pH 7.0, 50 mM) was incubated at 28 °C for 15 min and terminated by mixing with ethyl acetate/acetic acid (99:1). After extraction, the reaction products were analysed as mentioned in Section F. The control reactions were carried out under the same conditions but without FAD or NADPH, or NADPH was replaced with NADH (1 mM).

Synthesis of rishirilide A (1) from 5 catalyzed by RslO9 and RslO8. An assay mixture (100 µL) containing RslO9 (5 µM) and RslO8 (10 µM), compound **5** (100 µM), NADPH (1 mM) and Tris buffer (pH7.5, 50 mM) was incubated at 28 ̊C for 15 min. The enzymatic reaction was extracted, evaporated and metabolites profile was analysed by HPLC.

Time-course reaction of compound 5 with RslO9 to detect intermediate 6 during rishirilide D formation. An assay mixture containing RslO9 (5 µM), compound **5** (100 µM), NADPH (1 mM) and Tris buffer (pH7.0, 50 mM) was incubated at 28 °C. After incubation for 1, 1.5, 2, 2.5 and 3 min, a sample aliquot (50 µL) was taken and mixed with 500 µL of ethyl acetate/acetic acid (99:1). Organic phase containing extracted intermediates was evaporated and applied for HPLC analysis.

Enzymatic formation of 6 in large scale. The RslO9-catalyzed conversion of **5** was scaled up to 15 mL and carried out for 1 min at 28 °C. After extraction with ethyl acetate/acetic acid (99:1), the organic phase was evaporated and the resulting extract was purified by semi-preparative HPLC with the method described for compound **3** (Section F). Compound **6** was dissolved in 70 µL of DMSO. Then, 2 µL of **6** was incubated with either RslO9 (5 µM) or RslO8 (10 µM) as well as NADPH (1 mM) in Tris buffer (pH7.0, 50 mM) for 1 and 15 min at 28 °C. The enzymatic reactions were then extracted, the organic solvents evaporated, and the compounds analyzed by HPLC.

RslO9-catalyzed conversion of rishirilide A (1) into B (2). An assay mixture containing rishirilide A (**1**, 100 µM), NADPH (1 mM), Tris buffer (pH 7.0, 50 mM) and RslO9 (15 µM) was incubated at 28 °C. The enzymatic reaction was extracted, evaporated and analysed for rishirilide B (**2**) formation by HPLC.

^{18}O-labeling reaction of compound 5 with RslO9 and RslO8. The dixygen in solution A (Tris pH 7.5, 50 mM, 5 µM RslO9 and 10 µM RslO8) and solution B (100 µM compound **5**, 1 mM NADPH and water) was thoroughly removed by 10 cycles of treatment with vacuum and nitrogen gas. Solution B was added to solution A in an anaerobic chamber and the reaction was started by injection of about 97% $^{18}O_2$ gas (Campro scientific). The reaction was incubated at room temperature for 5 minutes and then extracted [EtOAc:formic acid = 9:1 (*v*/*v*)]. The organic layer was filtered and the solvent was removed under reduced pressure. The residue was dissolved in MeOH before liquid chromatography-mass spectrometric analysis.

I. Identification of flavin cofactors bound to RslO5 and RslO9

Purified RslO5 (6.3 mg mL^{-1}, 200 µL) and RslO9 (23 mg mL^{-1}, 200 µL) were heat precipitated at 70 °C for 20 min, the pellets were removed by centrifugation, the supernatants were filtered and used for HPLC analysis.

The samples were analyzed on a UHPLC Thermo Fisher Scientific Ultimate 3000 SD system joined with a TSQ Quantum Access MAX ESI mass spectrometer. For the LC analysis, a Pursuit 3 PFP column (Agilent, 3 µm, 100 × 2 mm) was used (mobile phase A: water and mobile phase B: MeCN, both with 0.5% acetic acid (vol/vol) as a solvent modifier). The solvents were delivered at 0.5 mL/min under a gradient elution program: 0 min 97% A, 3 min 97% A, 5 min 5% A, 7 min 5% A, 7.3 min 97% A, 10 min 97% A. Full-scan mass spectra (m/z 200 - 1000) were collected in negative ESI mode, with an ion-spray voltage of 2500 V, ion source temperature of 320 °C. The pressures of sheath and auxiliary gas (N2) were set to 65 and 17 (arbitrary units), respectively. The ion transfer tube was heated up to 255 °C.

J. NMR data for compounds

NMR spectra are recorded using a Varian VNMR-S 600 or a Jeol ECZ 500 spectrometer. The Varian NMR spectrometer is equipped with 3 mm triple resonance inverse and 3 mm dual broadband probes, the Jeol NMR spectrometer is equipped with a Royal probe. Spectra were measured in CD_3OD or $CDCl_3$ at T = 25 °C or DMSO-d_6 at T = 35 °C. $CDCl_3$ contains 0.03 % TMS. TMS or residual solvent signals were used as an internal standard (for CD_3OD: δ_H = 3.30 ppm, δ_C = 49.0 ppm, for $CDCl_3$: TMS was used for proton calibration, solvent signal was used for calibration δ_C = 77.0 ppm, for DMSO-d_6: δ_H = 2.50 ppm, δ_C = 39.5 ppm).

Compound 1, rishirilide A

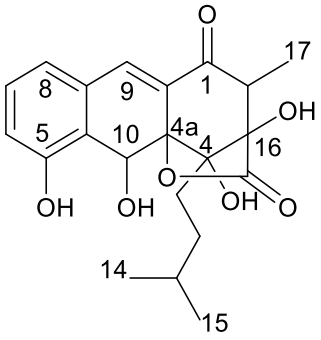

Rishirilide A (1), (calculated m/z = 387.145, $[M-H]^-$, observed m/z = 387.143, $[M-H]^-$), previously reported

NMR data (500/125MHz, 22°C, CD_3OD)

Pos.	**δ_C [ppm]**	**δ_H (*J* Hz) [ppm]**	**COSY**	**HMBC[a]**
1	199.5			2-H, 9-H, 10-H, 17-H_3
2	50.7	2.77 q (7.4)	17-H_3	^1J, 17-H_3
3	81.9			2-H, 17-H_3
4	82.2			11-H_a, 12-H_a
4a	85.4			9-H, 10-H, (11-H_a)
5	156.8			6-H, 7-H, 9-H, 10-H
6	120.8	6.98 d (8.0)	7-H, 8-H	^1J, 7-H, 8-H
7	131.1	7.24 t (7.8)	6-H, 8-H	
8	123.8	7.00 d (7.6)	6-H, 7-H	^1J
8a	131.8			7-H
9	139.6	7.57 s		8-H, ^1J
9a	132.0			9-H, 10-H
10	64.6	5.50 s		6-H, ^1J
10a	123.3			6-H, 9-H, (10-H)
11	31.0	H_a: 2.52 m	11-H_b, 12-H_a, 12-H_b	^1J, ^1J, 12-H_b, 13-H
		H_b: 1.63 m	11-H_a, 12-H_a, 12-H_b	
12	32.6	H_a: 1.60 m	11-H_a, 12-H_b, 13-H	11-H_a, 11-H_b, ^1J, 13-H, 14-H_3, 15-H_3
		H_b: 1.52 m	11-H_a, 12-H_a, 13-H	
13	30.0	1.41 m	12-H_a, 12-H_b, 14-H_3, 15-H_3	11-H_a, 11-H_b, 12-H_b
14	22.7	0.86 d (6.5)	13-H, 15-H_3	12-H_a, 12-H_b, 13-H, 15-H_3
15	23.2	0.89 d (6.5)	13-H, 14-H_3	12-H_a, 12-H_b, 13-H, 14-H_3
16	177.6			2-H
17	12.6	1.21 d (7.5)	2-H	2-H, ^1J

[a]weak signals in brackets

Compound 2, rishirilide B

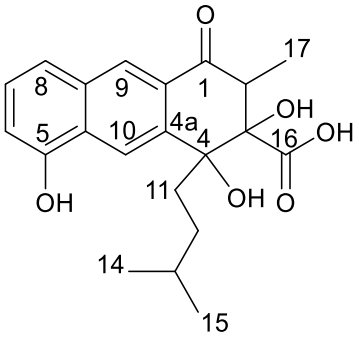

Rishirilide B (2), (calculated m/z = 371.149, $[M-H]^-$, observed m/z = 371.149, $[M-H]^-$), previously reported

NMR data (600/150MHz, 35°C, DMSO-d_6)

Pos.	**δ_C [ppm]**	**δ_H (*J* Hz) [ppm]**	**COSY[a]**	**HMBC[a]**
1	197.1			9-H, 2-H, 17-H_3
2	47.9	2.99 q (6.8)	17-H_3	17-H_3
3	83.6			2-H, 17-H_3
4	76.9			10-H, (11-H_a)
4a	140.0			9-H, (11-H_a)
5	153.0			6-H, 7-H, 8-H, 10-H
6	109.9	6.93 d (7.6)	7-H	8-H
7	126.3	7.28 dd (8.3, 7.6)	6-H, 8-H	6-H, 8-H
8	119.7	7.46 d (8.3)	7-H	6-H, 9-H
8a	132.3			7-H, 8-H, 10-H
9	125.7	8.29 s	(8-H)	8-H
9a	129.9			10-H
10	119.6	8.28 s		6-H, 9-H
10a	126.1			6-H, 8-H, 9-H
11	35.0	11-H_a: 2.23 dt (13.1, 3.9)	11-H_b, 12-H_a, 12-H_b	12-H_b
		11-H_b: 1.61 ddd (13.3, 12.8, 4.7)	11-H_a, 12-H_a, 12-H_b	
12	31.1	12-H_a: 1.38 m	11-H_a, 11-H_b	11-H_b, 13-H, 14-H_3, 15-H_3
		12-H_b: 0.78 m	11-H_a, 11-H_b, 13-H	
13	27.8	1.30 m	12-H_b, 14-H_3, 15-H_3	12-H_a, 14-H_3, 15-H_3
14	22.4	0.66 d (6.5)	13-H	15-H_3
15	22.6	0.77 d (6.5)	13-H	12-H_a, 13-H, 14-H_3
16	174.0			2-H
17	10.1	1.19 d (6.8)	2-H	2-H
OH		10.2 s br		

[a]weak signals in brackets

Compound 3, rishirilide D

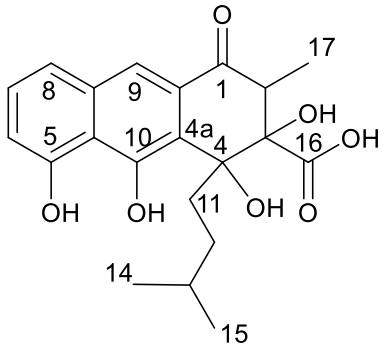

Rishirilide D (3), (calculated m/z = 387.145, $[M-H]^-$, observed m/z = 387.144, $[M-H]^-$), newly isolated compound

NMR Data (600/150MHz, 25°C, CD_3OD)

Pos.	**δ_C [ppm]**	**δ_H (*J* Hz) [ppm]**	**COSY**	**HMBC[a]**
1	199.0			2-H, 9-H, 17-H_3
2	49.5	2.99 q (6.8)	17-H_3	2-H
3	84.9			2-H, 17-H_3
4	82.8			11-H_a
4a	118.9			9-H, (11-H_a)
5	156.2			(6-H), 7-H
6	113.0	6.83 dd (8.0, 1.0)	7-H, 8-H	8-H
7	129.0	7.32 dd (8.0, 7.6)	6-H, 8-H	
8	121.7	7.36 dd (7.4, 1.0)	6-H, 7-H	6-H, 9-H
8a	136.1			7-H, 8-H, 9-H
9	121.2	8.01 s		8-H
9a	131.6[b]			
10	154.0			(9-H)
10a	118.0			6-H, 8-H, 9-H
11	37.6	H_a: 2.48 m[c]	11-H_b, 12-H_a, 12-H_b	12-H_a, 12-H_b, 14-H
		H_b: 1.85 m[c]	11-H_a, 12-H_a, 12-H_b	
12	33.2	H_a: 1.56 m[c]	11-H_a, 11-H_b, 12-H_b	11-H_a, 11-H_b, 13-H, 14-H_3, 15-H_3
		H_b: 1.18 m[c]	11-H_a, 11-H_b, 12-H_a	
13	29.8	1.41 m[c]	14-H_3, 15-H_3	11-H_a, 12-H_a, 12-H_b, 14-H_3, 15-H_3
14	23.0	0.85 d (6.4) [c]	13-H, 15-H_3	12-H_a, 12-H_b, 13-H, 15-H_3
15	23.0	0.75 d (6.4) [c]	13-H, 14-H_3	12-H_a, 12-H_b, 13-H, 14-H_3
16	175.6			2-H
17	10.5	1.27 d (6.8)	2-H	^{1}J, 2-H

[a]weak signals in brackets
[b]Not sure
[c]TOCSY proves this as one spinsystem

Compound 4

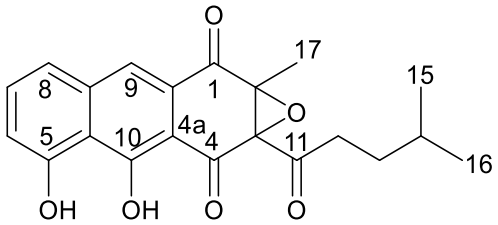

4, (calculated m/z = 367.119, $[M-H]^-$, observed m/z = 367.117, $[M-H]^-$), newly isolated compound

NMR data (600/150MHz, 25°C, CD_3OD)

Pos.	**δ_C [ppm]**	**δ_H (*J* Hz) [ppm]**	**COSY**	**HMBC[a]**
1	189.5			9-H, 17-H_3
2	66.6			17-H_3
3	71.2			17-H_3
4	195.5			(9-H, 17-H_3)
4a	108.3			9-H
5	159.1			6-H, 7-H, (8-H, 9-H)
6	116.1	7.01 d (7.9)	7-H	6-H, 9-H
7	134.5	7.61 t (7.9)	6-H, 8-H	^{1}J, 8-H
8	122.7	7.43 d (7.9)	7-H	6-H, 7-H, 9-H
8a	139.4			7-H, 8-H, 9-H
9	123.3	7.89 s		8-H
9a	127.8			9-H, (17-H_3)
10	165.3 br			(6-H, 8-H, 9-H)
10a	116.5			6-H, 9-H
11	203.2			12-H_a, 12-H_b, 13-H
12	40.7	H_a: 2.91 ddd (18.4, 7.8, 7.1)	12-H_b, 13-H_2	13-H, 14-H
		H_b: 2.71 ddd (18.4, 8.6, 6.8)	12-H_a, 13-H_2	
13	32.6	1.58 m	12-H_a, 12-H_b, 14-H	12-H_a, 12-H_b, 14-H, 15-H_3, 16-H_3
14	28.7	1.63 m	13-H_2, 15-H_3, 16-H_3	12-H_a, 12-H_b, 13-H, 15-H_3, 16-H_3
15	22.7	0.95 d (6.4)	14-H	13-H, 14-H, 16-H_3
16	22.8	0.95 d (6.4)	14-H	13-H, 14-H, 15-H_3
17	12.4	1.52 s		^{1}J

[a]weak signals in brackets

Compound 5

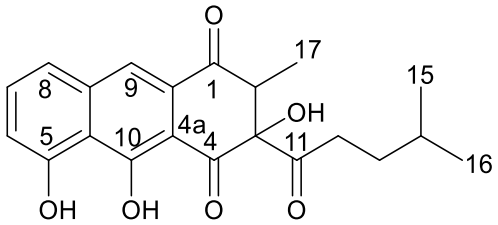

5, (calculated m/z = 369.134, $[M-H]^-$, observed m/z = 369.133, $[M-H]^-$), newly isolated compound

Double signal set in NMR spectra due to diastereomers **5a** and **5b**:
Ratio of **5a** / **5b** = 1.5 : 1 (based on integrals for protons 2-H)

NMR data for 5a (600/150MHz, 25°C, $CDCl_3$)

Pos.	**δ_C [ppm]**	**δ_H (*J* Hz) [ppm]**	**COSY**	**HMBC[a]**	**TOCSY**
1	193.6			2-H, 9-H, 17-H_3	
2	50.6	3.33 q (7.2)	17-H_3	17-H_3	17-H_3
3	87.8			2-H, 17-H_3	
4	197.5			2-H, 9-H, 10-OH	
4a	114.7			9-H, 10-OH	
5	158.0			6-H, 7-H, 8-H, (9-H)	
5-OH		9.33 br s			
6	115.0	7.09 (8.4)	7-H	8-H	7-H, 8-H
7	134.0	7.66 (8.0)	6-H, 8-H	5-OH, ^1J	6-H, 8-H
8	121.83	7.48 (8.0)	7-H	6-H, 9-H	6-H, 7-H
8a	138.84			(6-H), 7-H, 9-H, (10-OH)	
9	121.3	8.08 s		8-H, ^1J	
9a	128.74			2-H, 9-H	
10	164.2			9-H, 10-OH	
10-OH		14.2 br s			
10a	107.3			9-H, 10-OH	
11	208.5			2-H, 12-H_a, 12-H_b, 13-H_b, 17-H_3	
12	35.3	H_a: 2.85 ddd (18.5, 9.4, 5.6)	12-H_b, 13-H_a, 13-H_b	13-H_a	12-H_b, 13-H_a, 13-H_b, 15-H_3, 16-H_3
		H_b: 2.55 m	12-H_a		12-H_a, 13-H_a, 13-H_b, 14-H, 15-H_3, 16-H_3
13	31.8	H_a: 1.48 m	12-H_a, 12-H_b	12-H_a, 12-H_b, 14-H, 15-H_3, 16-H_3	12-H_a, 12-H_b, 15-H_3, 16-H_3
		H_b: 1.37 m	12-H_a, 12-H_b		12-H_a, 12-H_b, 13-H_a, 14-H, 15-H_3, 16-H_3
14	27.5	1.50 m	15-H_3, 16-H_3,	12-H_a, 12-H_b, 13-H_a, 15-H_3, 16-H_3	12-H_a, 12-H_b, 15-H_3, 16-H_3
15	22.18	0.85 d (6.4)	14-H	13-H_a, 13-H_b, 14-H, 16-H_3	12-H_a, 12-H_b, 13-H_a, 13-H_b, 14-H, 16-H_3
16	22.23	0.85 d (6.4)	14-H	13-H_a, 13-H_b, 14-H, 15-H_3	12-H_a, 13-H_a, 13-H_a, 13-H_b, 14-H, 15-H_3

17	12.0	1.20 (7.2)	2-H	2-H, ^{1}J	2-H

NMR Data for 5b (600/150MHz, 25°C, $CDCl_3$)

Pos.	**δ_C [ppm]**	**δ_H (*J* Hz) [ppm]**	**COSY**	**HMBC[a]**	**TOCSY**
1	191.5			2-H, 9-H, 17-H_3	
2	52.5	3.04 q (6.4)	17-H_3	17-H_3	17-H_3
3	89.4			2-H, 17-H_3	
4	193.6			2-H, 9-H, 17-H_3	
4a	107.4			9-H, 10-OH	
5	157.9			5-OH, 6-H, 7-H, 8-H	
5-OH		9.33 br s			
6	114.7	7.07 d (8.4)	7-H	8-H	7-H, 8-H
7	134.1	7.66 t (8.0)	6-H, 8-H	5-OH, ^{1}J	6-H, 8-H
8	121.78	7.48 d (8.0)	7-H	6-H, 9-H	6-H, 7-H
8a	138.81			(6-H), 7-H, 8-H, 9-H, (10-OH)	
9	120.2	8.09 s		8-H	
9a	130.85			9-H	
10	164.5			9-H, 10-OH	
10-OH		14.2 br s			
10a	107.4			9-H, 10-OH	
11	208.5			2-H, 12-H_a, 12-H_b, 13-H_a, 17-H_3	
12	34.6	H_a: 2.80 ddd (18.5, 9.2, 5.6)	12-H_b, 13-H_a, 13-H_b	13-H_a	12-H_b, 13-H_a, 13-H_b, 15-H_3, 16-H_3
		H_b: 2.56 m	12-H_a		12-H_a, 13-H_a, 13-H_b, 14-H, 15-H_3, 16-H_3
13	31.4	H_a: 1.39 m	12-H_a, 12-H_b	12-H_a, 12-H_b, 14-H, 15-H_3, 16-H_3	12-H_a, 12-H_b, 15-H_3, 16-H_3
		H_b: 1.28 m	12-H_a, 12-H_b		12-H_a, 12-H_b, 13-H_a, 14-H, 15-H_3, 16-H_3
14	27.36	1.46 m	15-H_3, 16-H_3,		12-H_a, 12-H_b, 15-H_3, 16-H_3
15	22.17	0.83 (6.4)	14-H	13-H_a, 13-H_b, 14-H, 16-H_3	12-H_a, 12-H_b, 13-H_a, 13-H_b, 14-H, 16-H_3
16	22.19	0.83 (6.4)	14-H	13-H_a, 13-H_b, 14-H, 15-H_3	12-H_a, 13-H_a, 13-H_a, 13-H_b, 14-H, 15-H_3
17	8.7	1.34 d (6.8)	2-H	2-H, ^{1}J	2-H

[a]weak signals in brackets

K. Supporting Figures

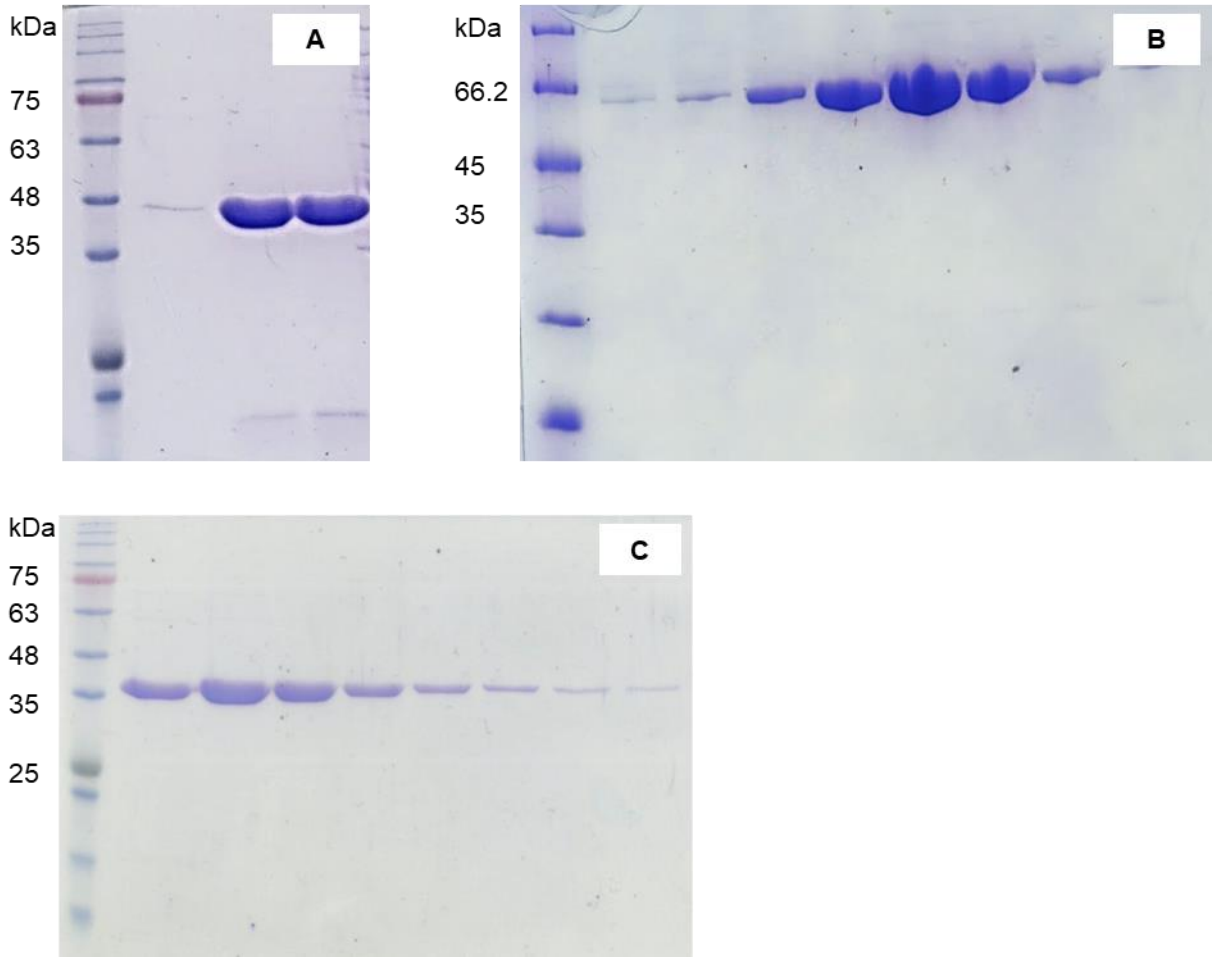

Figure S1. SDS-PAGE gel of purified proteins.
The protein samples (1 to 20 µg) of (A) RslO5, (B) RslO9 and (C) RslO8 were analysed after size exclusion chromatography.

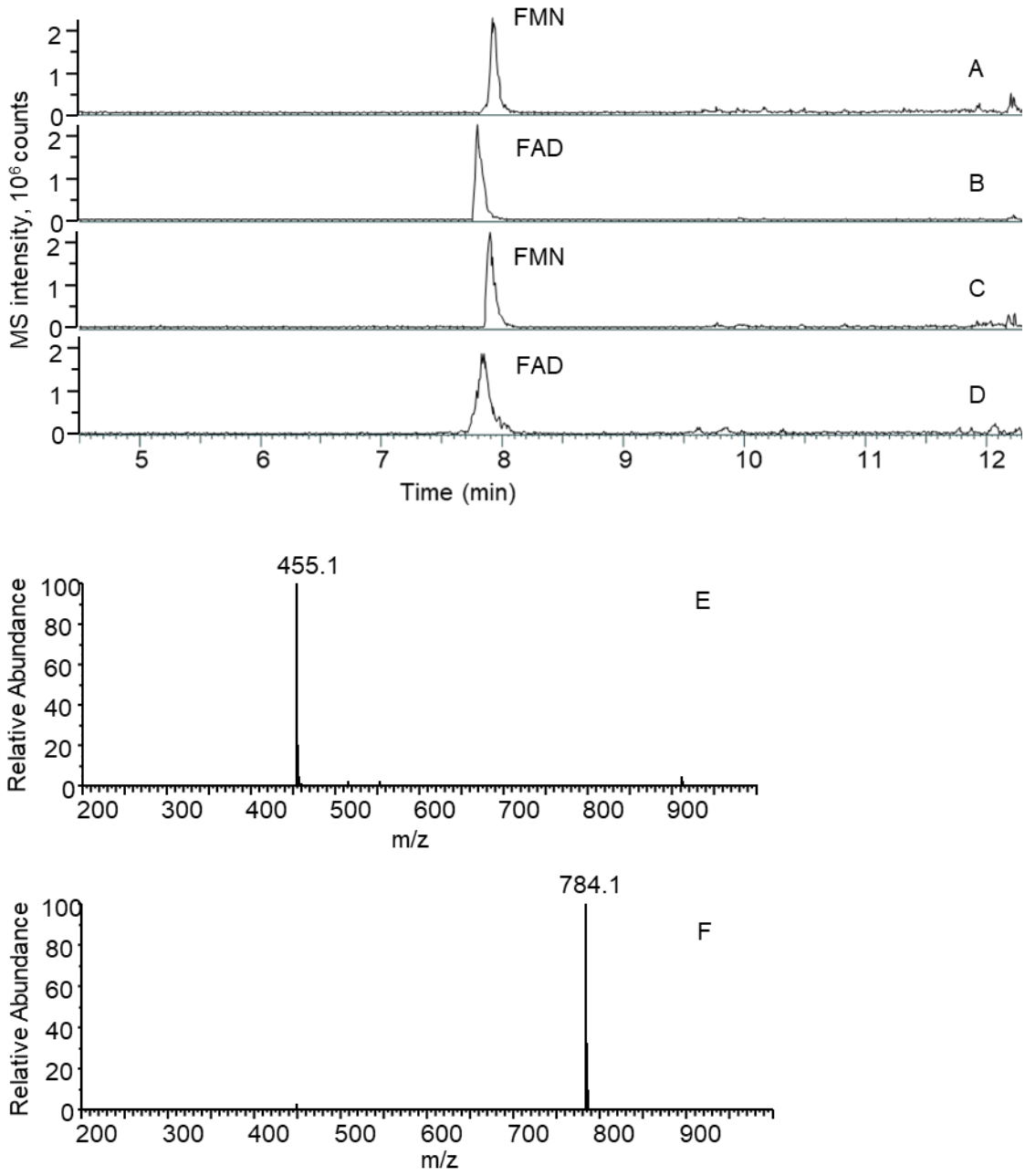

Figure S2. LC-MS (TIC) analysis of flavin cofactors released from RslO5 and RslO9 upon heat denaturation. (A) FMN standard; (B) FAD standard; (C) FMN released from RslO5; (D) FAD released from RslO9; (E) MS spectrum of a peak corresponding to FMN cofactor released from RslO5; (F) MS spectrum of a peak corresponding to FAD cofactor released from RslO9.

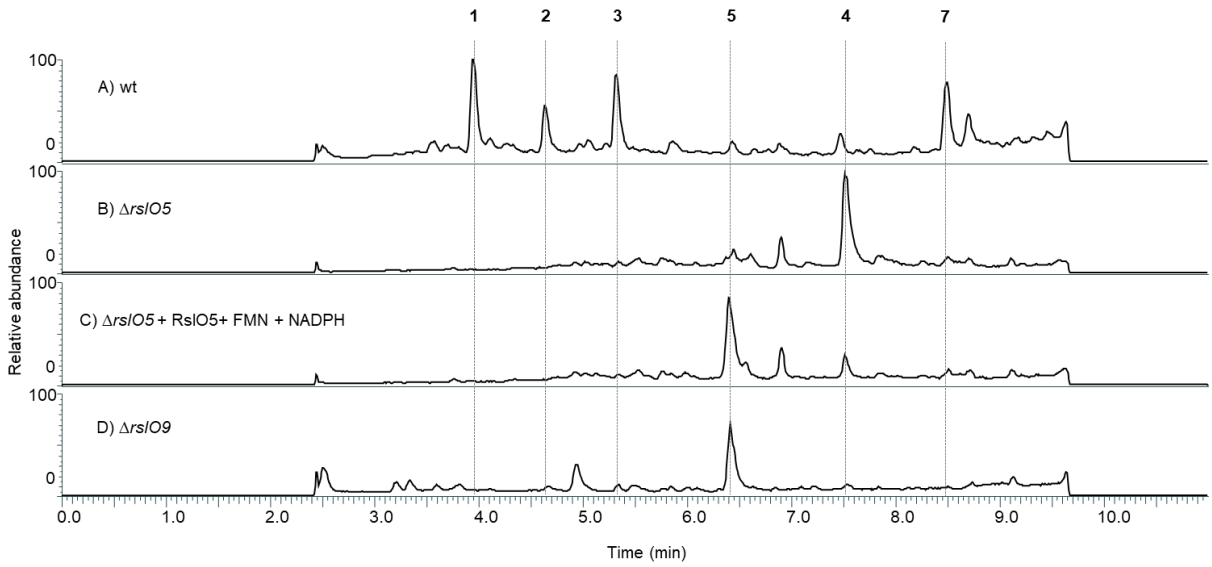

Figure S3. Gene inactivation studies to probe the roles of *rslO5* and *rslO9*.
(A) TIC analysis of a culture extract from *S. bottropensis*. (B) Extract from *S. bottropensis* Δ*rslO5*. (C) Reaction of purified RslO5 with a crude extract from the Δ*rslO5* mutant with added FMN and NADPH. (D) Extract from *S. bottropensis* Δ*rslO9*. The compound at 4.7 min is a degradation product of **5** (structure not elucidated). The asterisks (*) mark a compound that is not related to rishirilide biosynthesis.

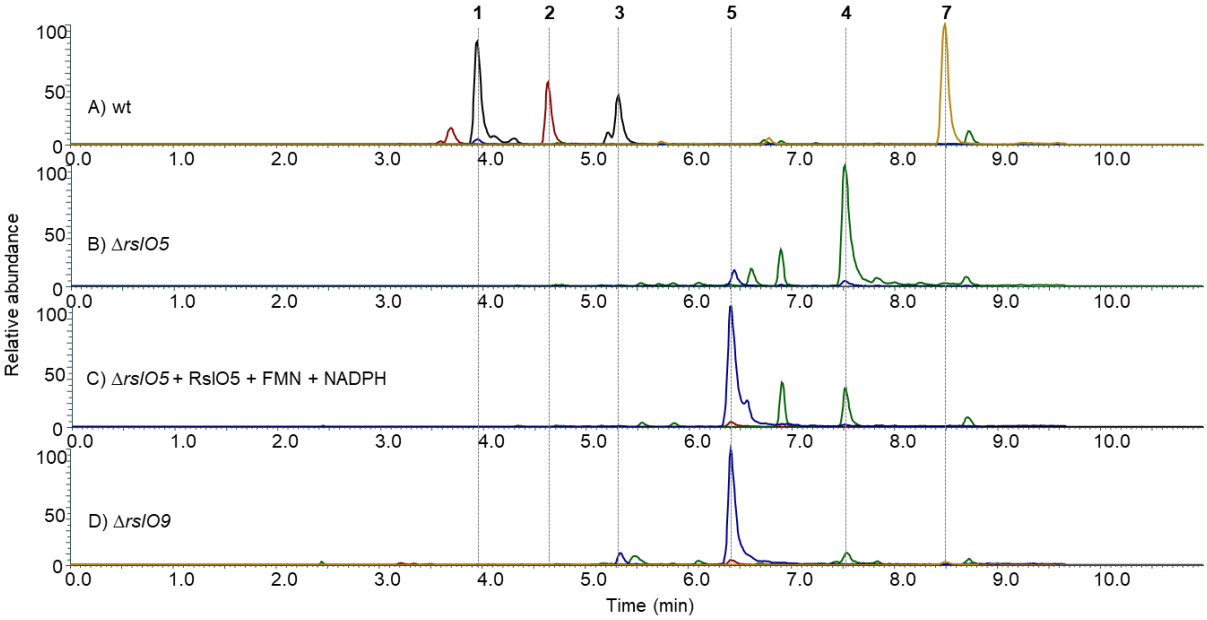

Figure S4. Gene inactivation studies to probe the roles of *rslO5* and *rslO9*.
EIC of m/z 387 $[M-H]^-$ (black, **1** and **3**), m/z 371 $[M-H]^-$ (red, **2**), m/z 367 $[M-H]^-$ (green, **4**), m/z 369 $[M-H]^-$ and m/z 339 $[M-H]^-$ (yellow, **7**) in (A) a culture extract from *S. bottropensis*; (B) extract from *S. bottropensis* Δ*rslO5*; (C) reaction of purified RslO5 with a crude extract from the Δ*rslO5* mutant with added FMN and NADPH; (D) extract from *S. bottropensis* Δ*rslO9*.

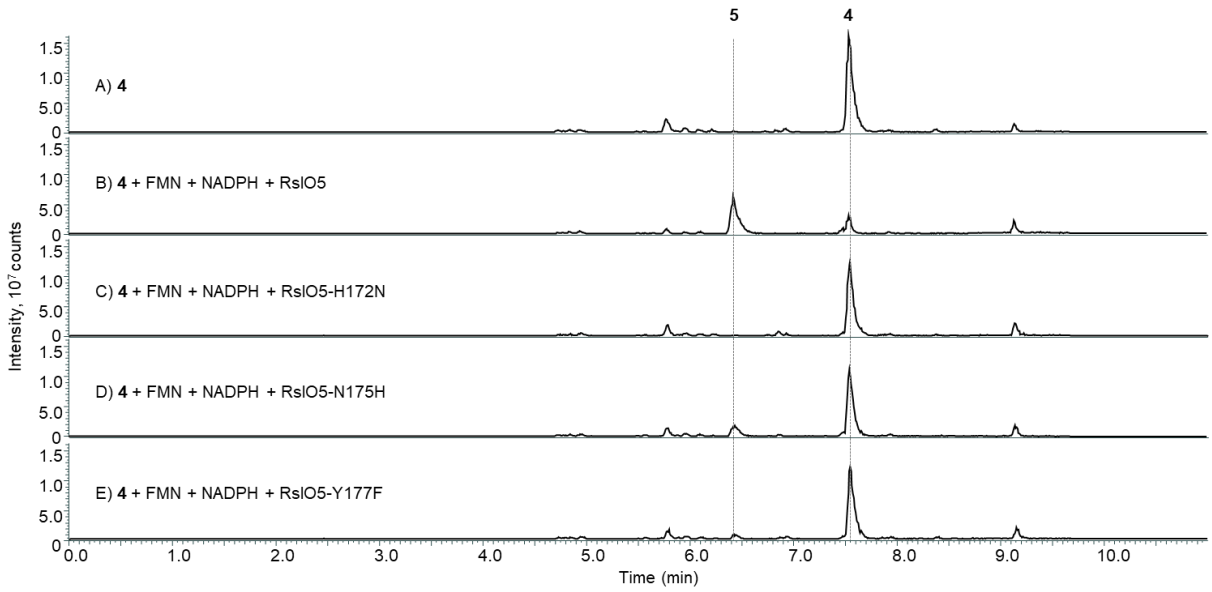

Figure S5. LC-MS (TIC) analysis of the reaction of RslO5 and active site variants with 4. (A) Purified **4**; (B) **4** + RslO5 + FMN + NADPH; (C) **4** + RslO5-H172N + FMN + NADPH; (D) **4** + RslO5-N175H + FMN + NADPH; (E) **4** + RslO5-Y177F + FMN + NADPH.

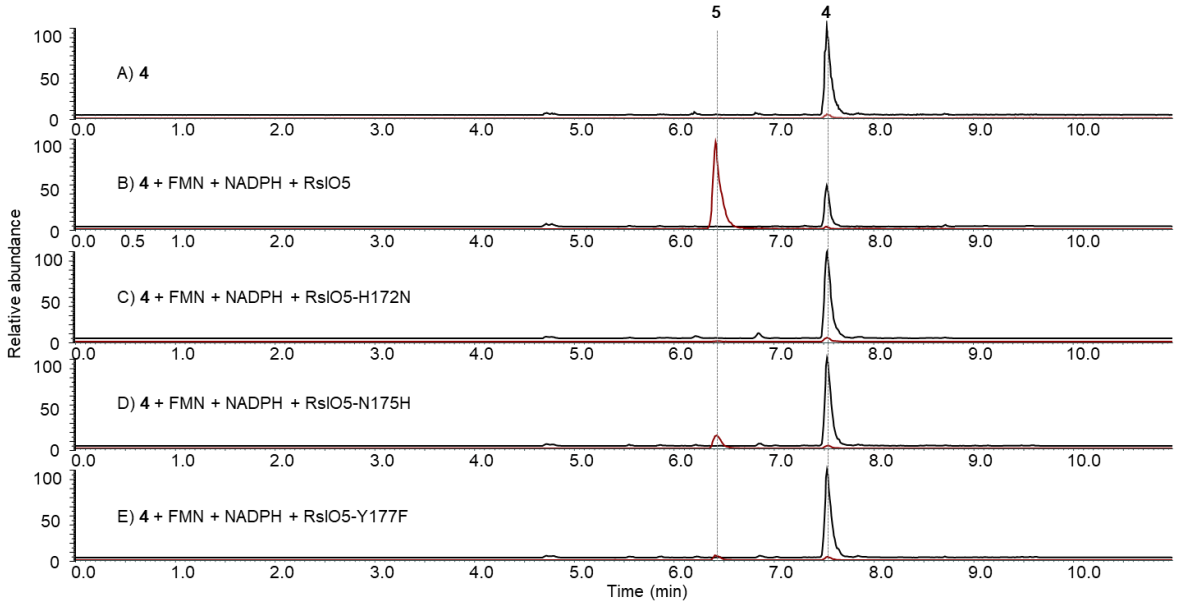

Figure S6. Reactions of RslO5 and active site variants with **4**. EIC of m/z 367 $[M-H]^-$ (black, **4**) and m/z 369 $[M-H]^-$ (red, **5**). (A) Purified **4**; (B) **4** + RslO5 + FMN + NADPH; (C) **4** + RslO5-H172N + FMN + NADPH; (D) **4** + RslO5-N175H + FMN + NADPH; (E) **4** + RslO5-Y177F + FMN + NADPH.

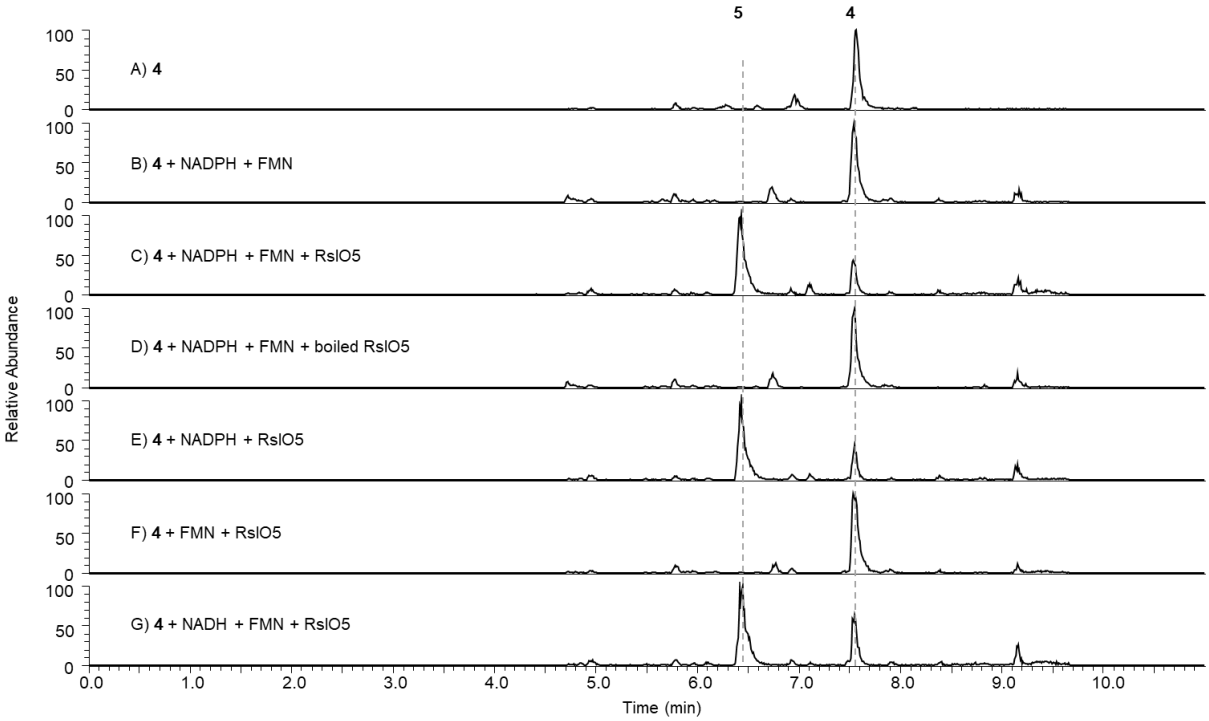

Figure S7. LC-MS (TIC) analysis of cofactor effects and controls of the RslO5-catalyzed reaction. (A) Purified **4**; (B) **4** + NADPH + FMN; (C) **4** + NADPH + FMN +RslO5; (D) **4** + NADPH + FMN + boiled RslO5; (E) **4** + NADPH + RslO5; (F) **4**+ FMN +RslO5; (G) **4** + NADH + FMN +RslO5.

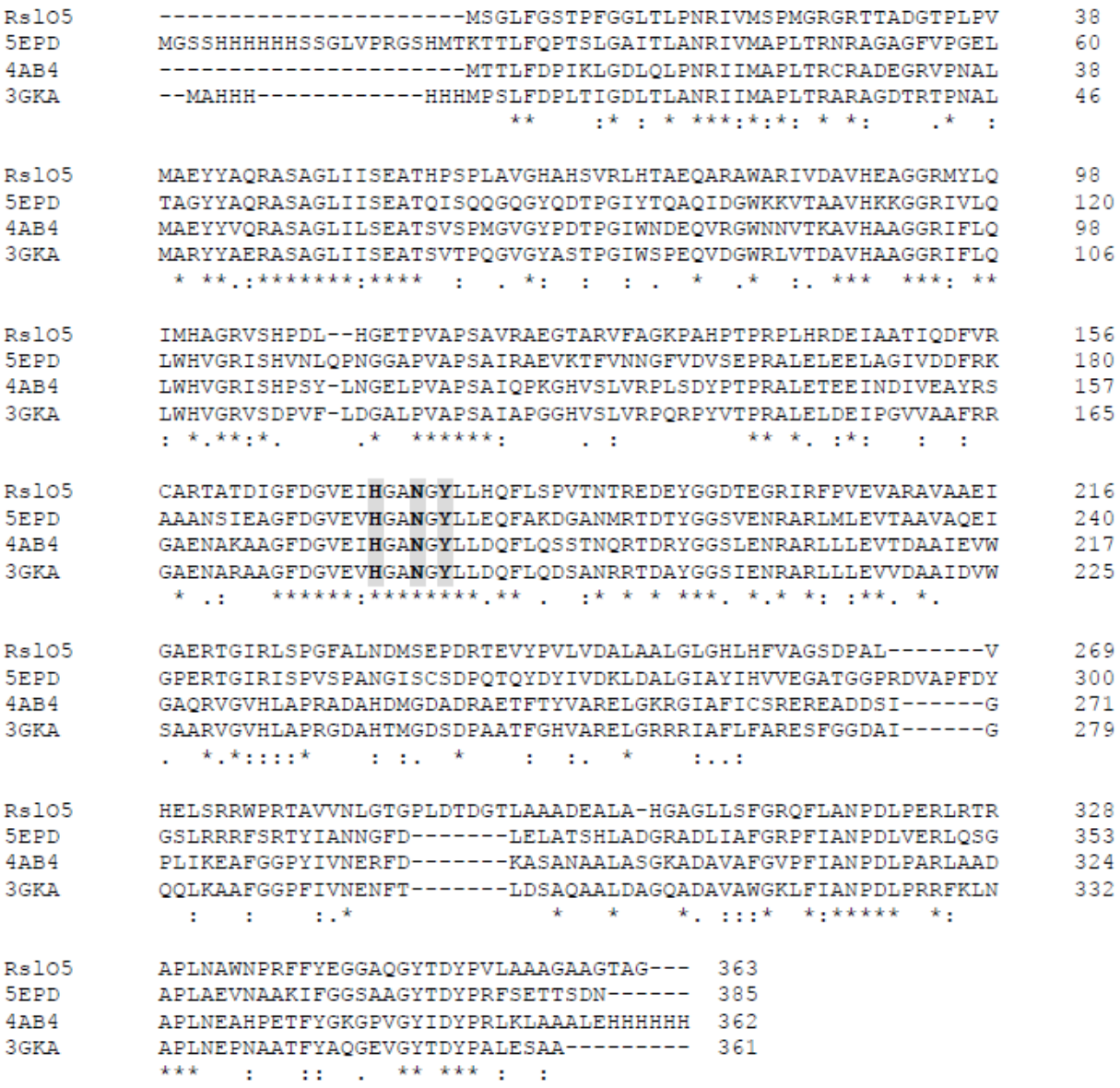

Figure S8. Multiple sequences alignment of RslO5 with the members of Old Yellow Enzyme family. 4AB4 - xenobiotic reductase B from *Pseudomonas putida*; 5EPD - glycerol trinitrate reductase XdpB from *Agrobacterium* sp. R89-1; 3GKA - N-Ethylmaleimidine reductase from *Burkholderia pseudomallei*. Proteins assigned with the accession numbers from Protein Data Bank. The putative active site residues are given in bold and highlighted.

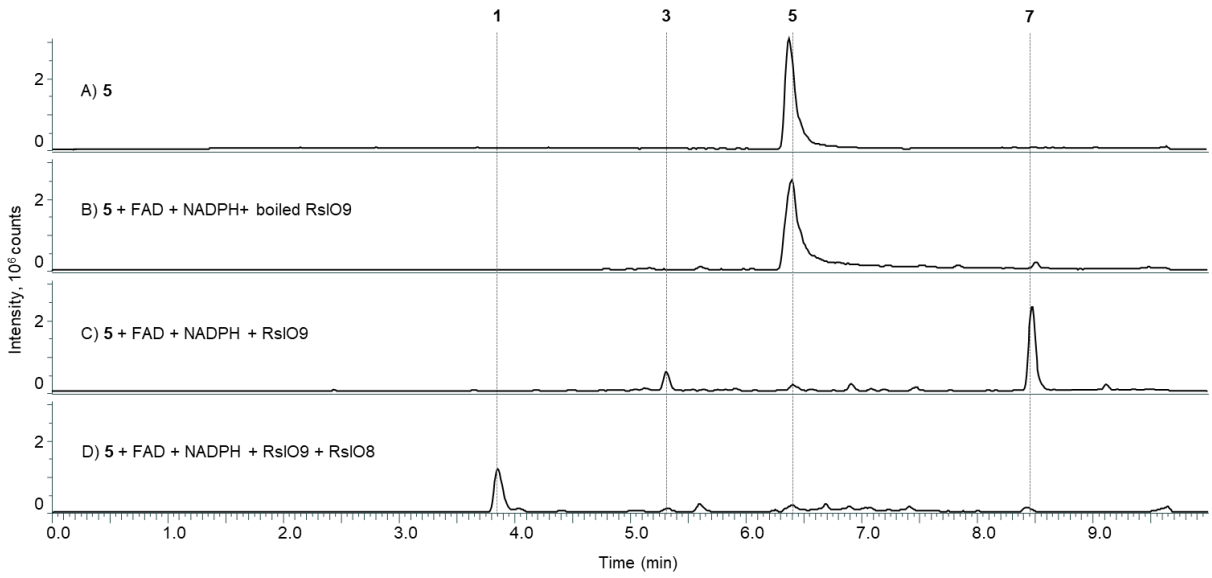

Figure S9. LC-MS (TIC) analysis of the reactions of RslO8 and RslO9 *in vitro*. (A) Chromatogram for purified **5**. (B) Incubation of **5** with heat inactivated RslO9. (C) Reaction of **5** with RslO9. (D) Reaction of **5** with RslO9 and RslO8. Reactions B, C, and D all included FAD and NADPH.

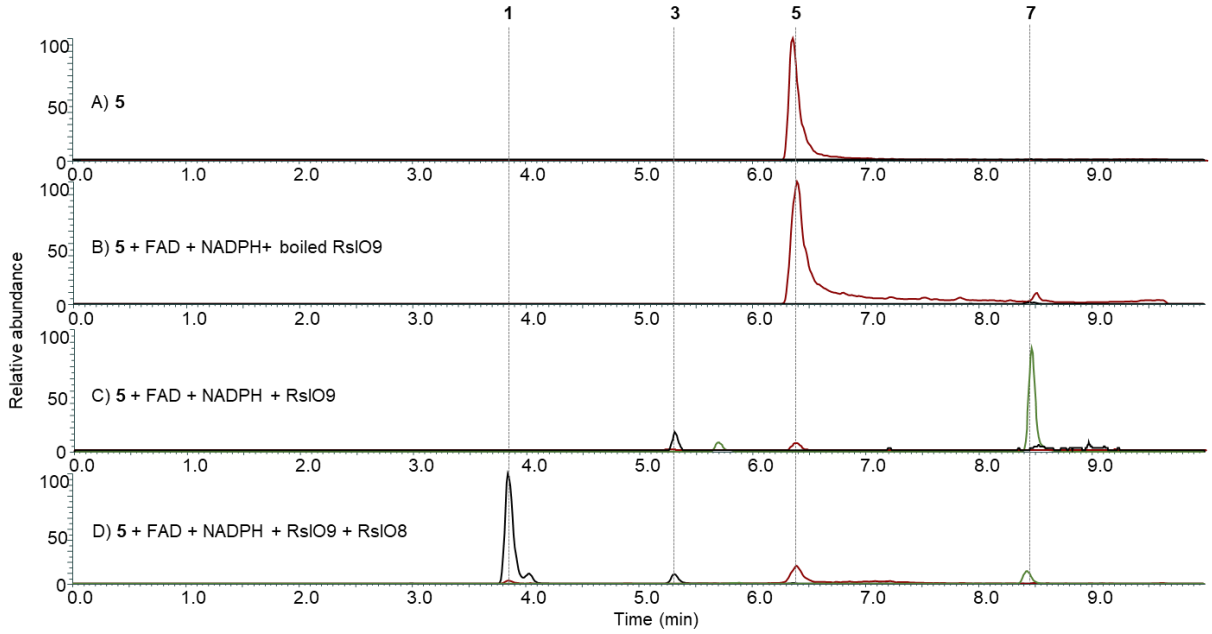

Figure S10. LC-MS analysis of the reactions of RslO8 and RslO9 *in vitro*. EIC of m/z 369 $[M-H]^-$ (**5**, red), m/z 387 $[M-H]^-$ (**1** and **3**, black) and m/z 339 $[M-H]^-$ (green, **7**). (A) Purified **5**. (B) Incubation of **5** with heat inactivated RslO9. (C) Reaction of **5** with RslO9. (D) Reaction of **5** with RslO9 and RslO8.

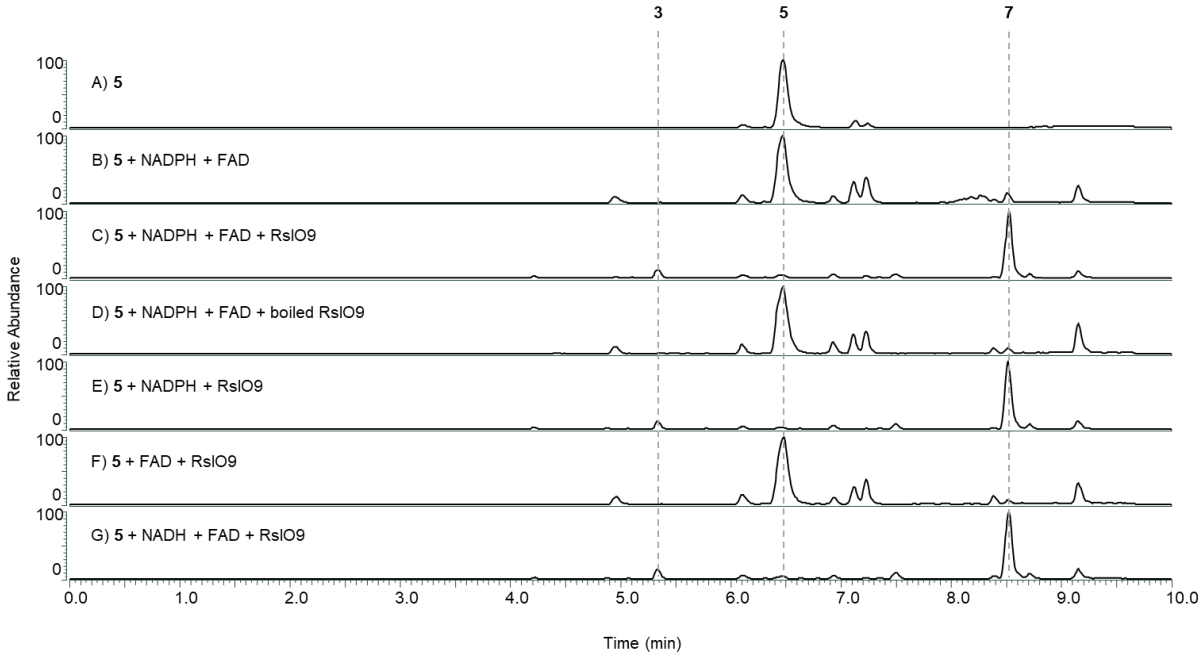

Figure S11. LC-MS (TIC) analysis of controls and cofactor effects on the RslO9-catalyzed reaction. (A) Purified **5**; (B) **5** + NADPH + FAD; (C) **5** + NADPH + FAD +RslO9; (D) **5** + NADPH + FAD + boiled RslO9; (E) **5** + NADPH + RslO9; (F) **5**+ FAD +RslO9; (G) **5** + NADH + FAD +RslO9.

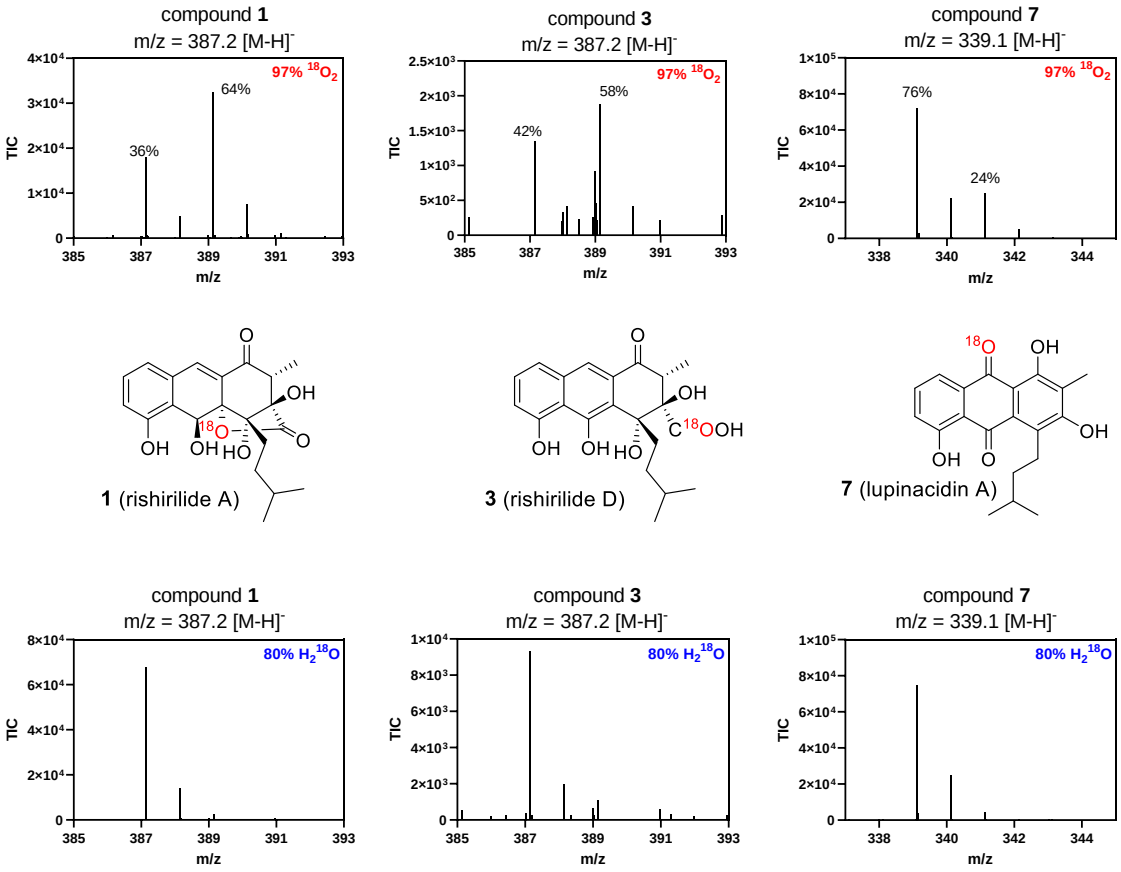

Figure S12. Isotope labeling assay of compound **5** incubated with RslO9 and RslO8 in presence of 97% $^{18}O_2$ gas or 80% $H_2{}^{18}O$ (*v*/*v*). Negative ion mode ESI MS measurement of compounds **1**, **3** and **7**. Three compounds show an incorporation of a single ^{18}O-atom. When labeled water was used, the incubation time was 2 min and direct extraction of the assay was required, because ketones spontaneously exchange oxygen with water. The results show no significant incorporation of ^{18}O.

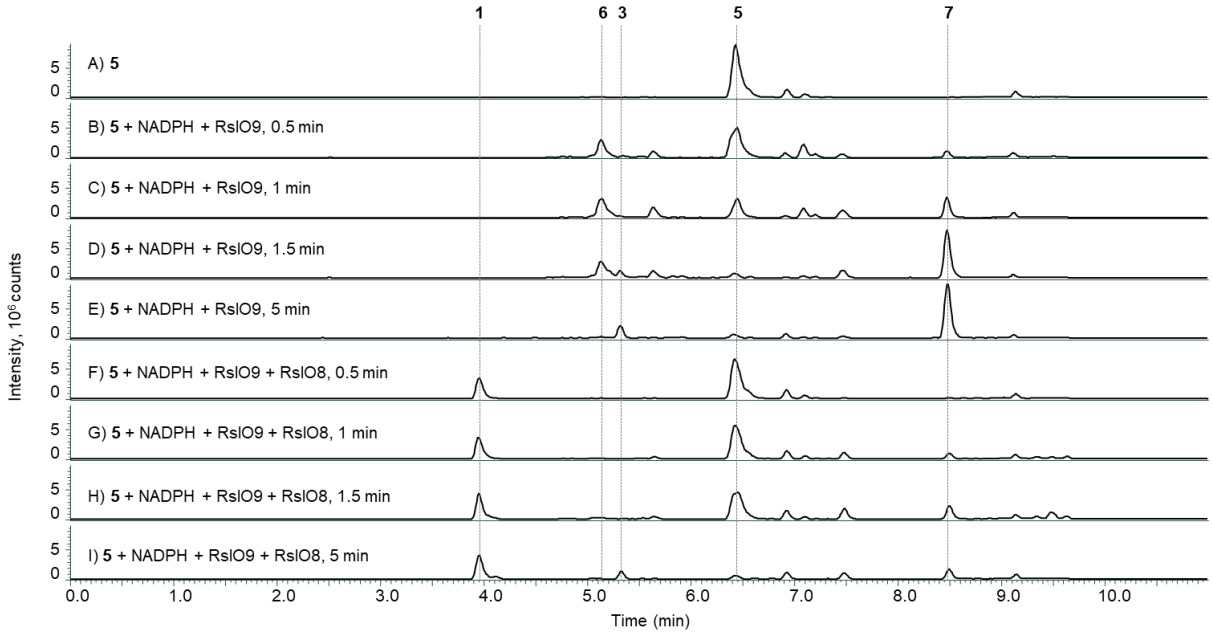

Figure S13. LC-MS (TIC) analysis of compound **6** formation during time-course reactions of RslO9 and RslO9 together with RslO8. (A) Chromatogram for purified **5**. (B) Incubation of **5** with RslO9 for 0.5 min, (C) 1 min, (D) 1.5 min and (E) 5 min. (F) Reaction of **5** with RslO9 and RslO8 incubated for 0.5 min, (G) 1 min, (H) 1.5 min and (I) 5 min.

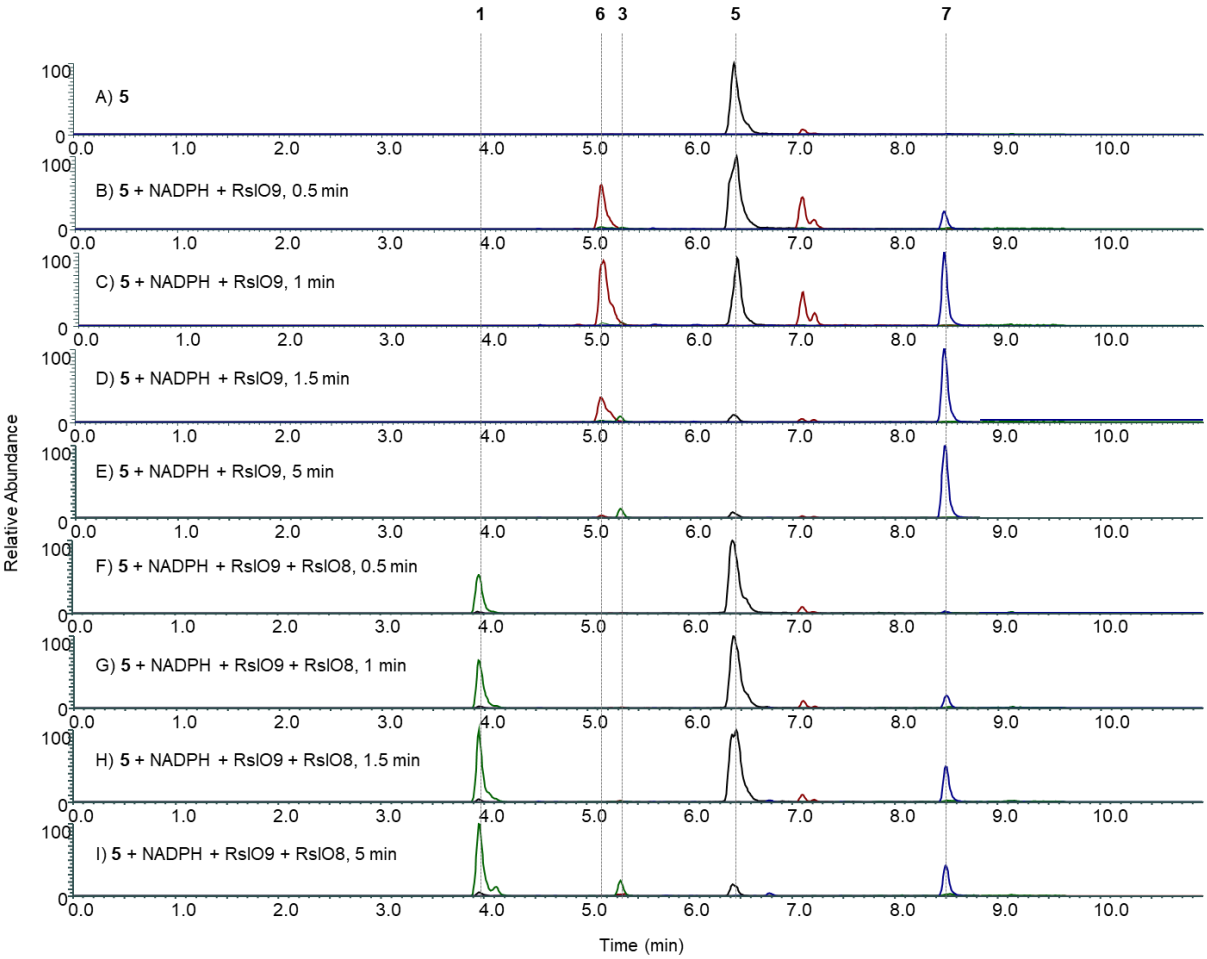

Figure S14. Detection of compound **6** formation during time-course reactions of RslO9 and RslO9 together with RslO8. EIC of m/z 369 $[M-H]^-$ (black, **5**), m/z 385 $[M-H]^-$ (red, **6**), m/z 387 $[M-H]^-$ (green, **1** and **3**) and m/z 339 $[M-H]^-$ (blue, **7**). (A) Purified **5**. (B) Incubation of **5** with RslO9 for 0.5 min, (C) 1min, (D) 1.5 min and (E) 5 min. (F) Reaction of **5** with RslO9 and RslO8 incubated for 0.5 min, (G) 1min, (H) 1.5 min and (I) 5 min.

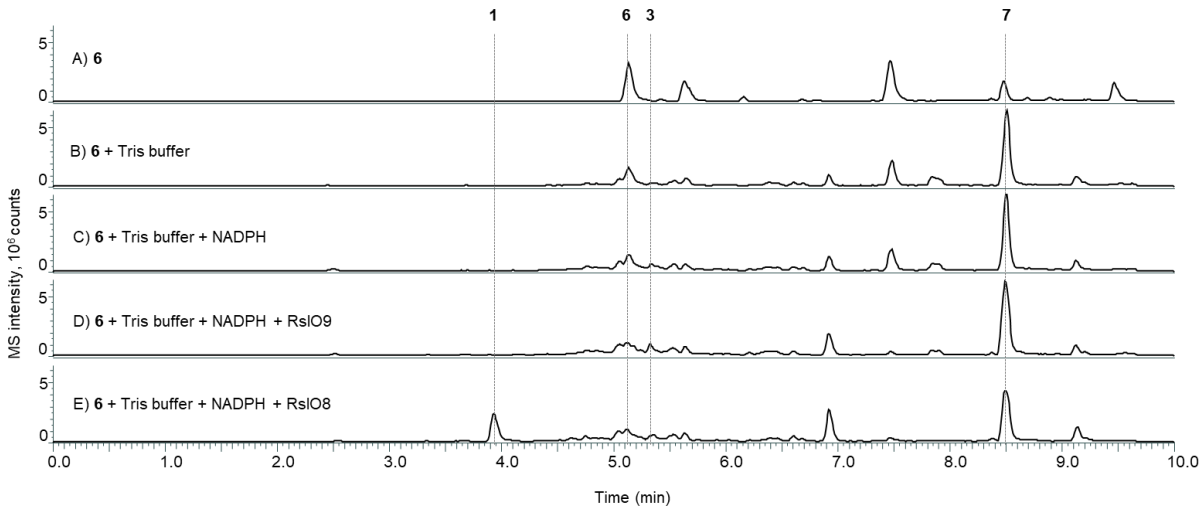

Figure S15. LC-MS (TIC) analysis of in vitro conversion of **6** into rishirilide D (**3**) or rishirilide A (**1**) catalyzed by RslO9 and RslO8, respectively. (A) Chromatogram for purified **6**. (B) Incubation of **6** in Tris buffer, pH 7.0 for 5 min; (C) Incubation of **6** in Tris buffer + NADPH; (D) **6** + NADPH + RslO9; (E) **6** + NADPH + RslO8.

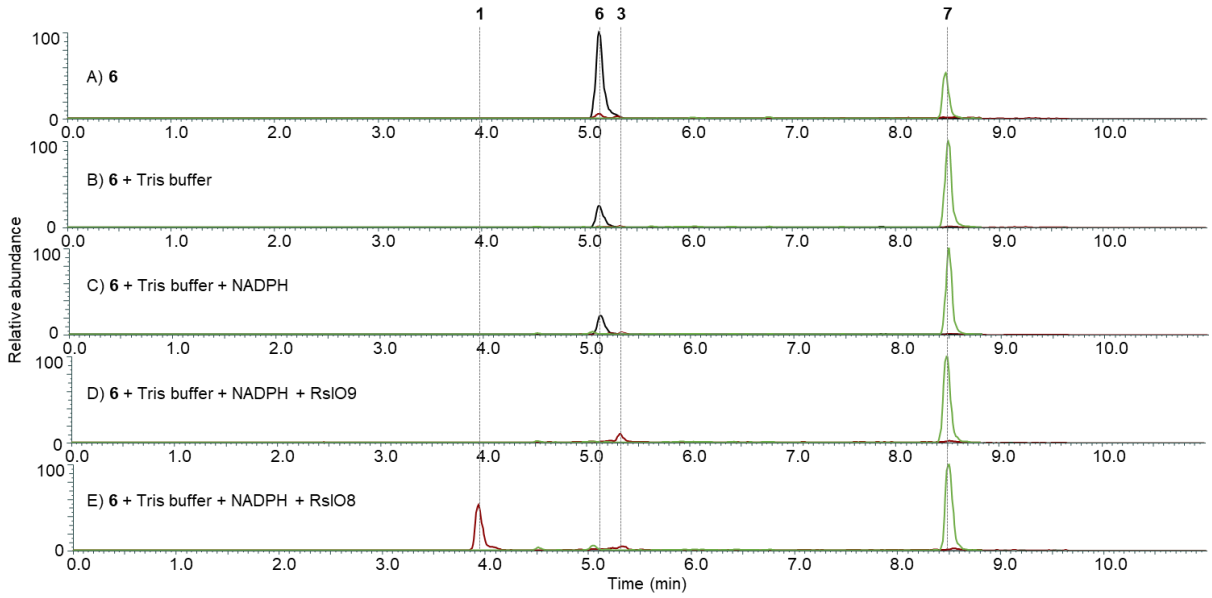

Figure S16. Reaction of *in vitro* conversion of **6** into rishirilide D (**3**) or rishirilide A (**1**) catalyzed by RslO9 and RslO8, respectively. EIC of m/z 385 $[M-H]^-$ (black, **6**), m/z 387 $[M-H]^-$ (red, **1** and **3**); m/z 339 $[M-H]^-$ (green, **7**). (A) Purified **6**. (B) Incubation of **6** in Tris buffer, pH7.0 for 5 min; (C) Incubation of **6** in Tris buffer + NADPH; (D) **6** + NADPH + RslO9; (E) **6** + NADPH + RslO8.

Collected **6** was quickly decomposed due to its instability. **7** may not only be generated from **3**, but possibly also from earlier intermediates, which requires further investigation.

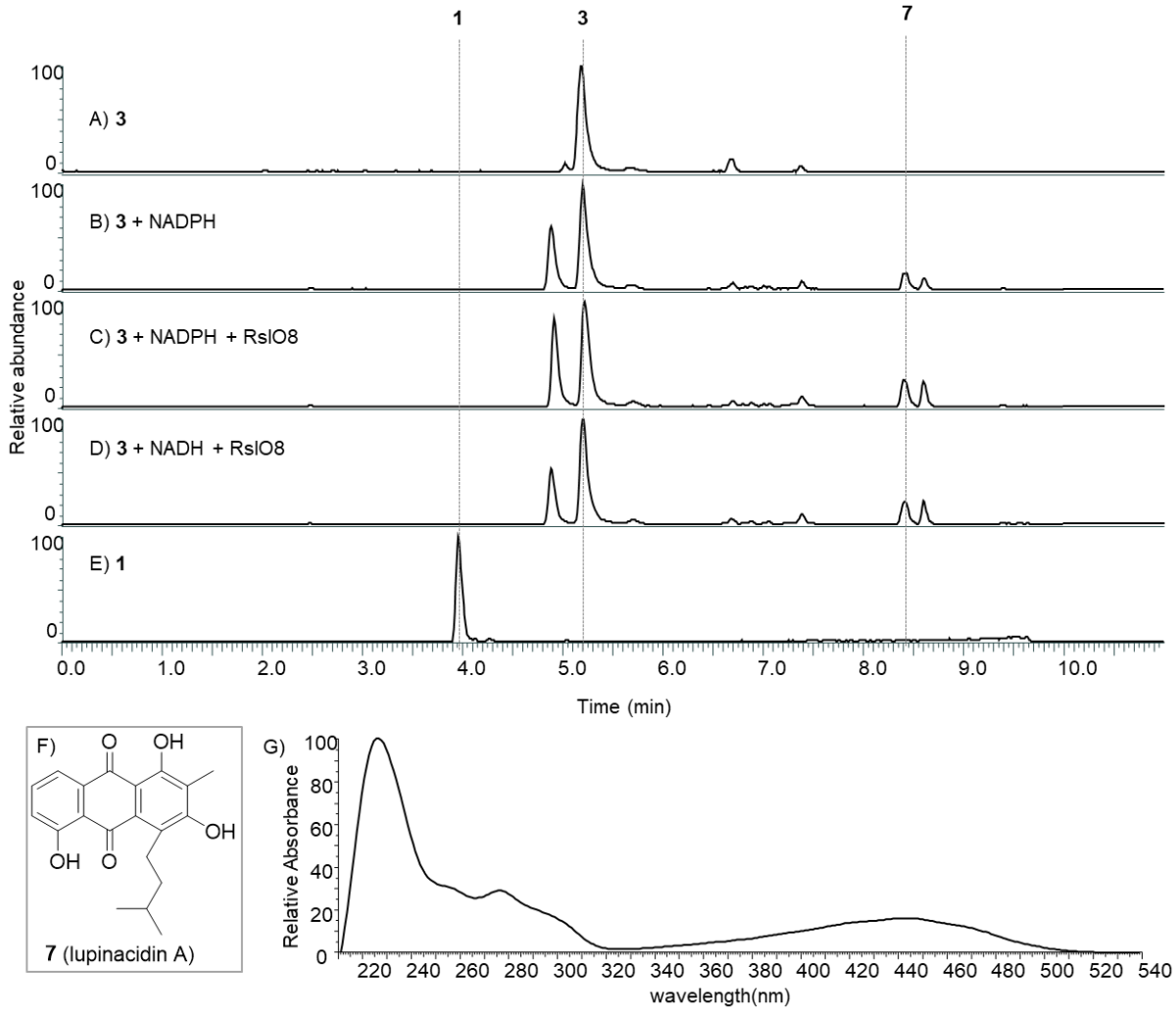

Figure S17. LC-MS analysis of the reactions of RslO8 and **3** *in vitro* (A) Purified **3**; (B) **3** + NADPH; (C) **3** + NADPH + RslO8; (D) **3** + NADH + RslO8; (E) Purified **1**; F) Structure of lupinacidin A; G) UV-Vis profile of compound **7** that is virtually identical to the previously reported spectrum of lupinacidin A.

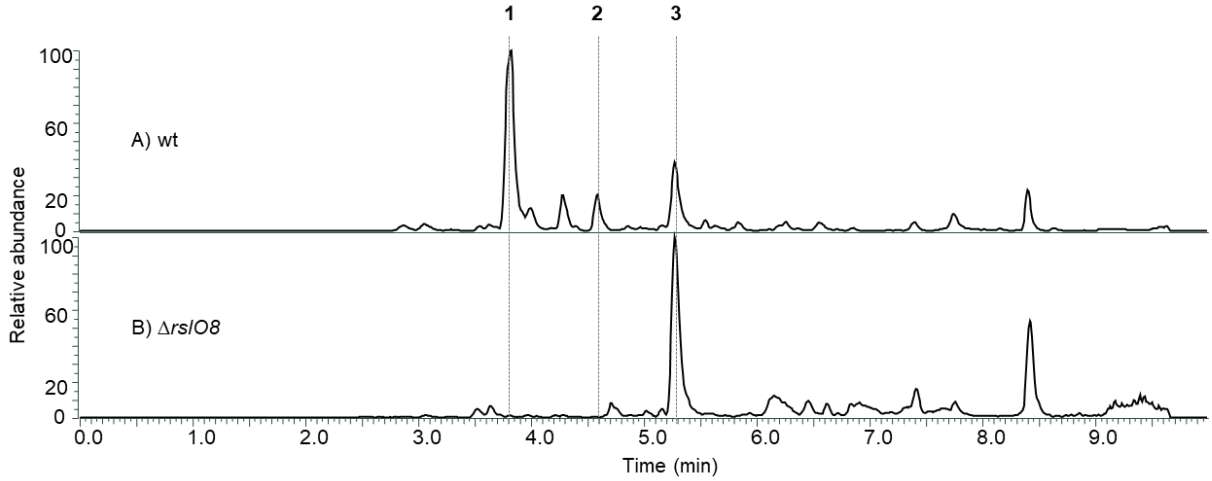

Figure S18. Gene inactivation studies to probe the role *rslO8*. (A) TIC analysis of a culture extract from *S. bottropensis*. (B) Extract from *S. bottropensis* Δ*rslO8.*

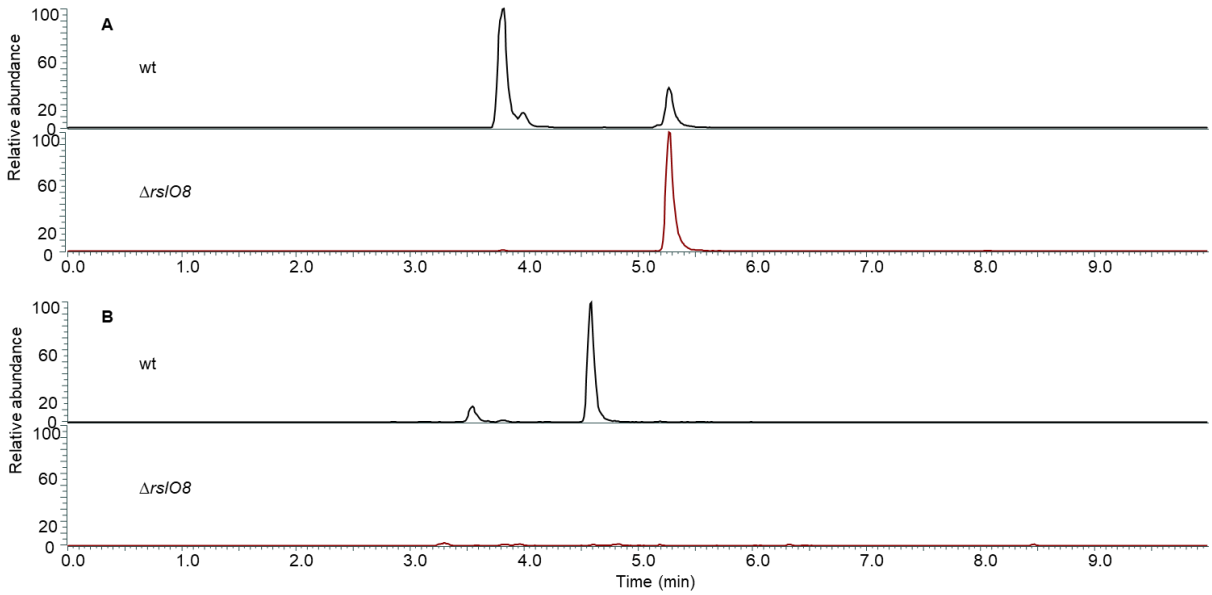

Figure S19. Gene inactivation studies to probe the role *rslO8*. (A) EIC of m/z 387 $[M-H]^-$ (**1** and **3**) in an extract from wild type *S. bottropensis* and Δ*rslO8.* (B) EIC of m/z 371 $[M-H]^-$ (**2**) in an extract from wild type *S. bottropensis* and Δ*rslO8.*

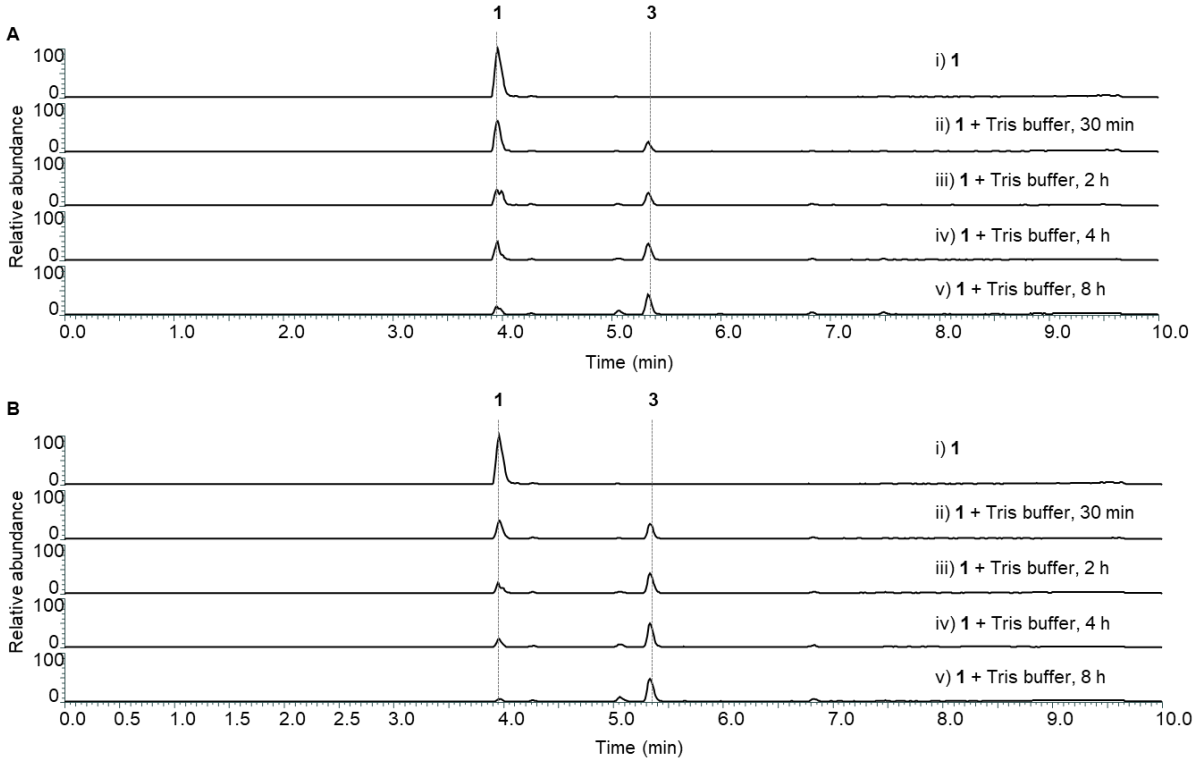

Figure S20. LC-MS (TIC) analysis of spontaneous conversion of rishirilide A (**1**) into rishirilide D (**3**). (A) Chromatogram of time-course conversion of **1** into **3** at pH7.5 and (B) at pH8.0. i) Purified **1**; ii) Incubation of **1** in Tris buffer at 28 °C and detection of **3** formation after 30 min, iii) 2 h, iv) 4 h and v) 8 h.

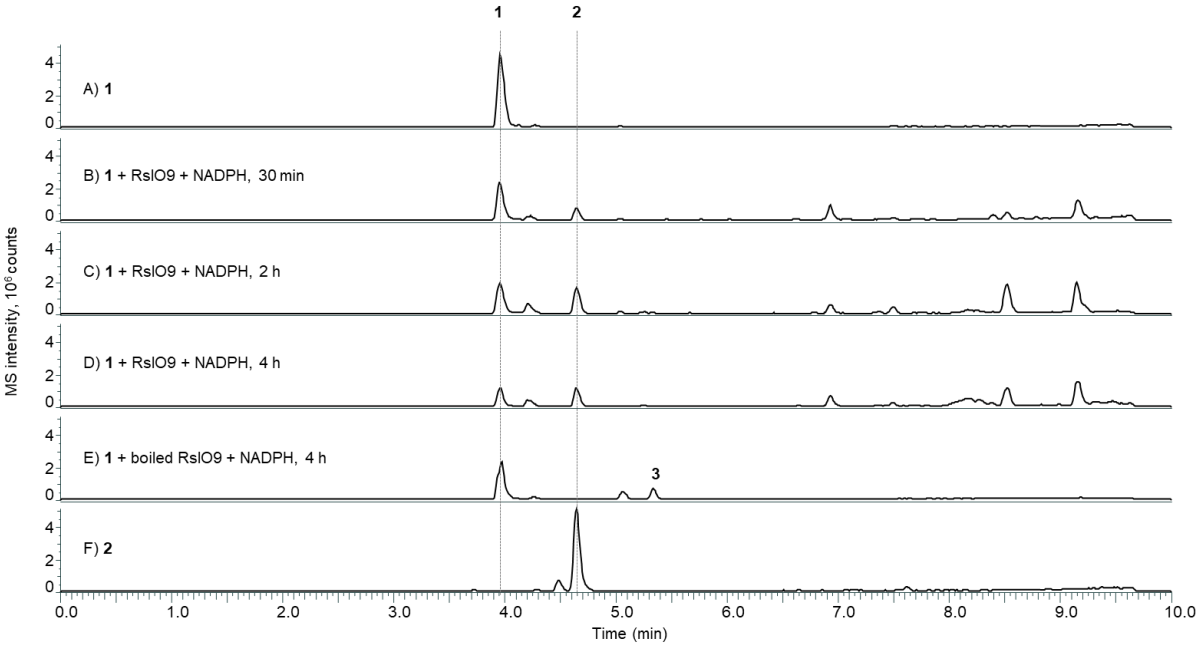

Figure S21. LC-MS (TIC) analysis of *in vitro* conversion of rishirilide A (**1**) into rishirilide B (**2**) catalyzed by RslO9. (A) Chromatogram for purified **1**. (B) Incubation of **1** with RslO9 and NADPH for 30 min, (C) 2 h, and (D) 4 h. (E) Control reaction of **1** with heat inactivated RslO9 and NADPH incubated for 4 h. (F) Purified **2**.

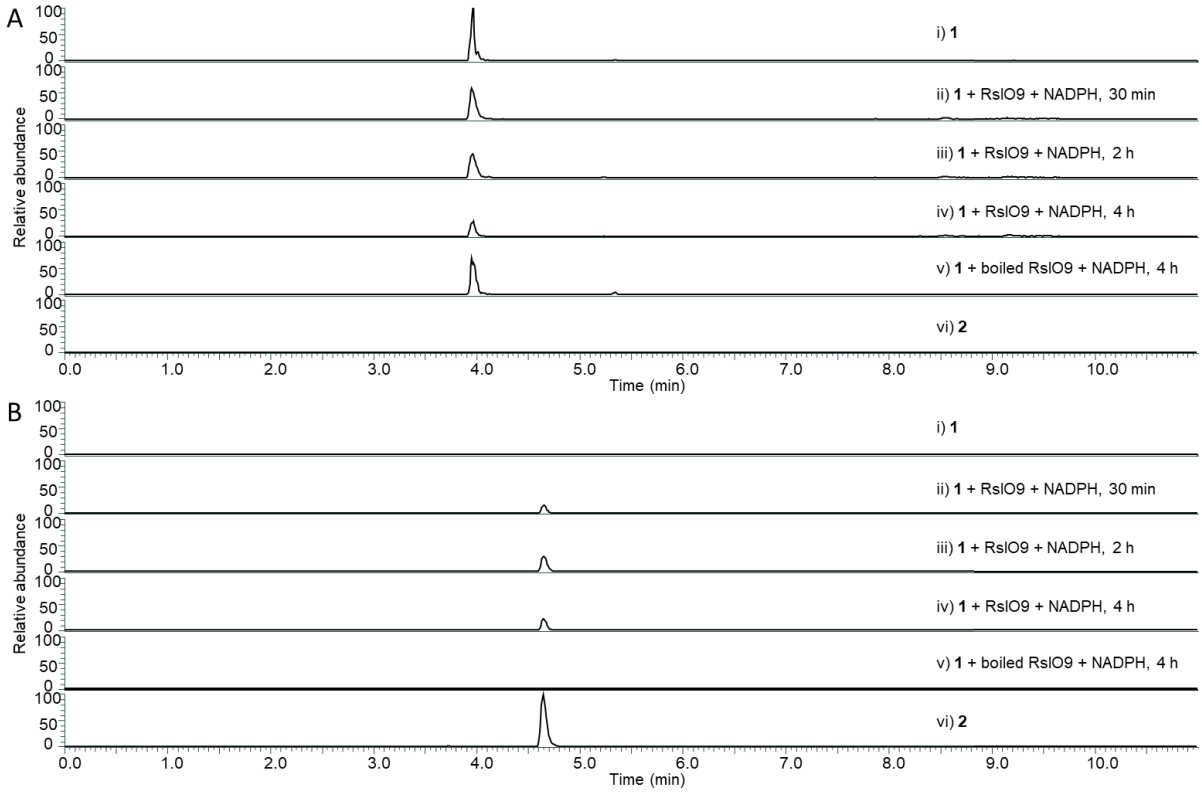

Figure S22. LC-MS analysis of the *in vitro* conversion of rishirilide A (**1**) into rishirilide B (**2**) catalyzed by RslO9. (A) EIC of m/z 387 $[M-H]^-$ (**1** and **3**). (B) EIC of m/z 371 $[M-H]^-$ (**2**). (i) Purified **1**. (ii) enzymatic reaction of **1** with RslO9 and NADPH for 30 min, (iii) 2 h, and (iv) 4 h. (v) Control reaction of **1** with heat inactivated RslO9 and NADPH incubated for 4 h. (vi) Purified **2**.

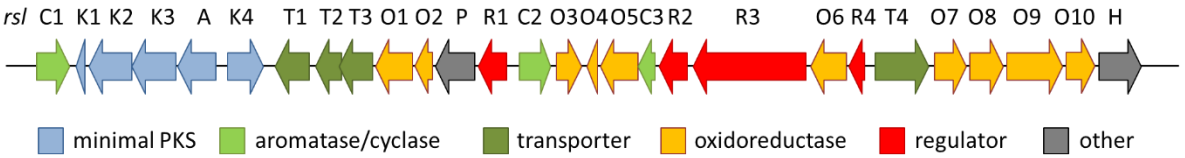

Protein	Proposed function
RslC1	Aromatase
RslK1	Acyl carrier protein
RslK2	Ketosynthase (β)
RslK3	Ketosynthase (α)
RslA	Acyl transferase
RslK4	3-oxo-acyl-ACP synthase III
RslT1	ABC-transporter (substrate binding)
RslT2	ABC-transporter (ATP-binding)
RslT3	ABC-transporter (transmembrane)
RslO1	Luciferase-like monooxygenase
RslO2	Flavin reductase
RslP	Phosphotransferase
RslR1	SARP family regulator
RslC2	Second ring cyclase
RslO3	3-oxoaxyl-ACP reductase
RslO4	Anthrone monooxygenase
RslO5	OYE NAD(P)H:flavin oxidoreductase
RslC3	Aromatase
RslR2	SARP family regulator
RslR3	LAL-family regulator
RslO6	Luciferase-like monooxygenase
RslR4	MarR-family regulator
RslT4	Drug resistance transporter (MFS)
RslO7	MDR superfamily oxidoreductase
RslO8	MDR superfamily oxidoreductase
RslO9	FAD-dependent monooxygenase
RslO10	C9-ketoreductase
RslH	Amidohydrolase

Figure S23. Rishirilide gene cluster and proposed functions of encoded proteins in *S. bottropensis*

Recently, wild-type strain *Streptomyces olivaceus* was reported to produce rishirilide B, C, lupinacidin A and galvaquinone B.[6] The rishirilide gene cluster was identified and a few structural genes were inactivated in this strain (the gene cluster was named *rsd* for this organism; below we show homologous *rsl* genes from *S. bottropensis* in brackets).

The deletion of ketosynthase β *rsdK2 (rslK2 homologue*) shut down biosynthesis completely as well as the inactivation of luciferase like monooxygenase (LLM) *rsdO1 (rslO1 homologue)*. Mutants deficient in amidohydrolase and LLM-encoding genes *rsdH* and *rsdO6*, respectively (*rslH* and *rslO6*) accumulated the same compounds as wild type. Inactivation of flavin

reductase *rsdO2 (rslO2)* led to accumulation of nonrearranged compounds – galvaquinone A and B.

Based on similarity to other type II PKS biosynthetic genes, *rslK1-K3* encode the minimal PKS and the acyl carrier protein. Likely, *rslO10* encodes the ketoreductase typically required for proper folding of the polyketide chain. In addition, aromatases encoded by RslC1- RslC3 most likely assist in the cyclization of the polyketide chain, whereas *rslR1- rslR4* likely encode pathway transcriptional regulators. The core redox tailoring enzyme (encoded by *rslO5*, *rslO8, rslO9*) were described in this work, other protein functions remain to be investigated.

MTQRARRPDPAAPPTPVPAPAPAPAPAPDETVPVLVAGAGPGGLSTAVFLGLHGVPA
LVVERHPGTSTAVKATGQYPHTMEALAIAGAAGTVRERGRAYRSDFHMVVAKTLA
GPVLRTLMSGDQLSMRHVSPEDWGTASQSAVESVLADRAAELGSRLRFSTRLTSLTQ
DADGVTAVTQHTGTGERRVIRARYLVVADGWRSGIRQSLGIEMRGRGTVGKVLRVL
FEADLSEPLSHTDGAADGRRFTALHVGRAVLFNTEIPGLYGYFRNLTPELPDGWWTN
EDTVAAQIRSDLGIPDIPLKIEEISETEISCGVAERFREGRALLVGDAAHVMPPTGGMG
GNTAYLDGLYLGWKLAAVLRGTAGEALLDSHDAERRPYAEELVEQQFANLVDRISP
ELADESLAVALPPPVVAFGYRFPKGAVLLEPDDDGELFEDPSRPTGRPGSHAPYVPLT
RRDGSATSTTALFGHAFVLLTGPDGAAWAEGALASADALGVAVQVHRVGPGSELLD
AEGAFSTAYGIGADGAALVRPDRFVAWRCTGTHPDPAAEIERALRHVLHRPAH

Figure S24. Protein sequence of RslO9 used in this work.

Figure S25. ^{1}H NMR of rishirilide A (**1**) **(**500MHz, 22°C, CD_3OD)

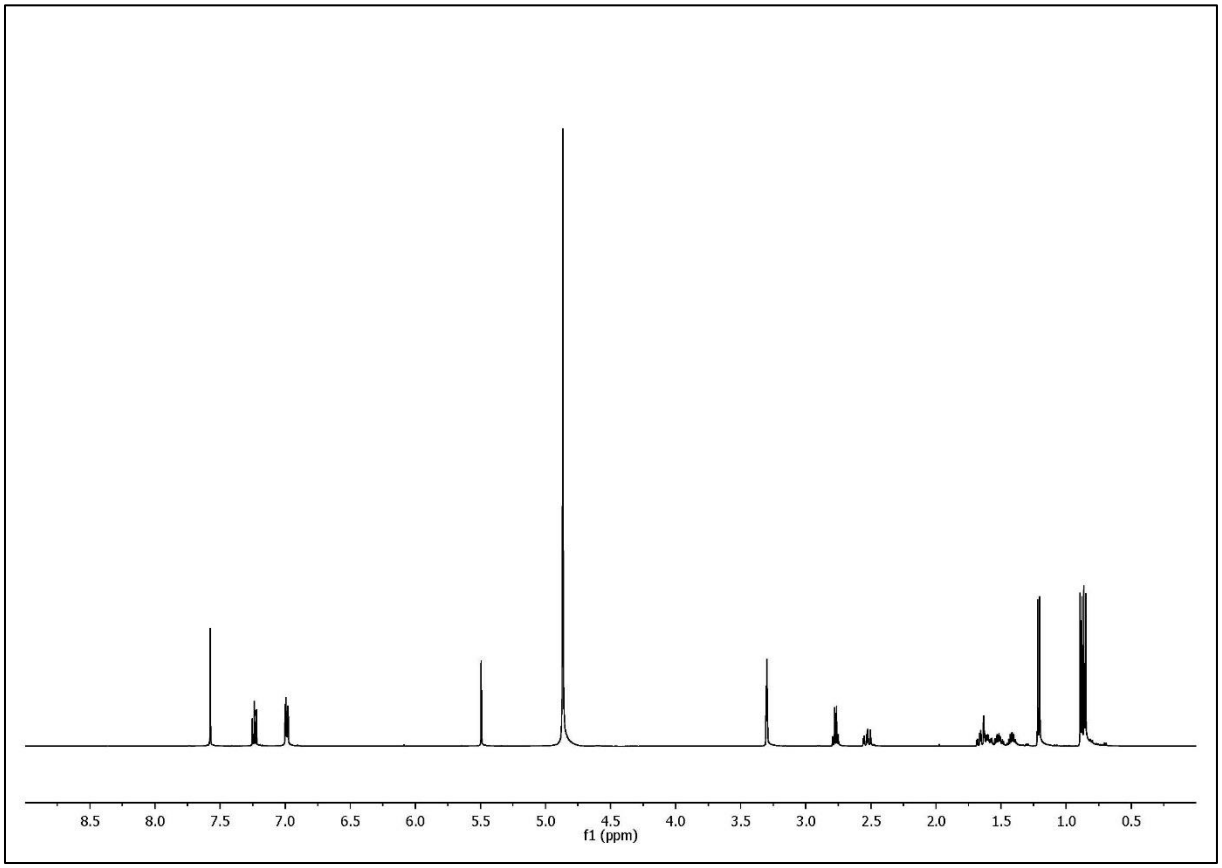

Figure S26. ^{13}C NMR of rishirilide A (**1**) **(**125MHz, 22°C, CD_3OD)

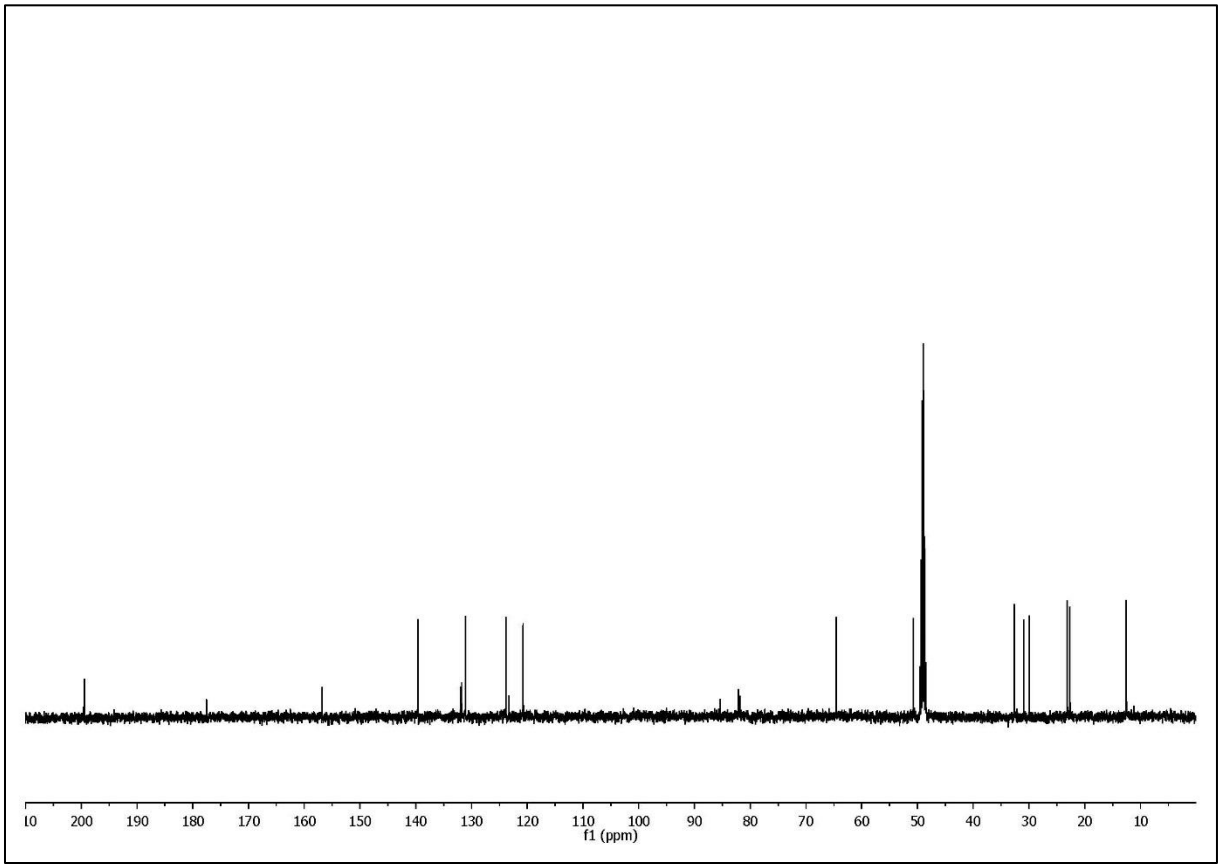

Figure S27. COSY NMR of rishirilide A (**1**) **(**500MHz, 22°C, CD_3OD)

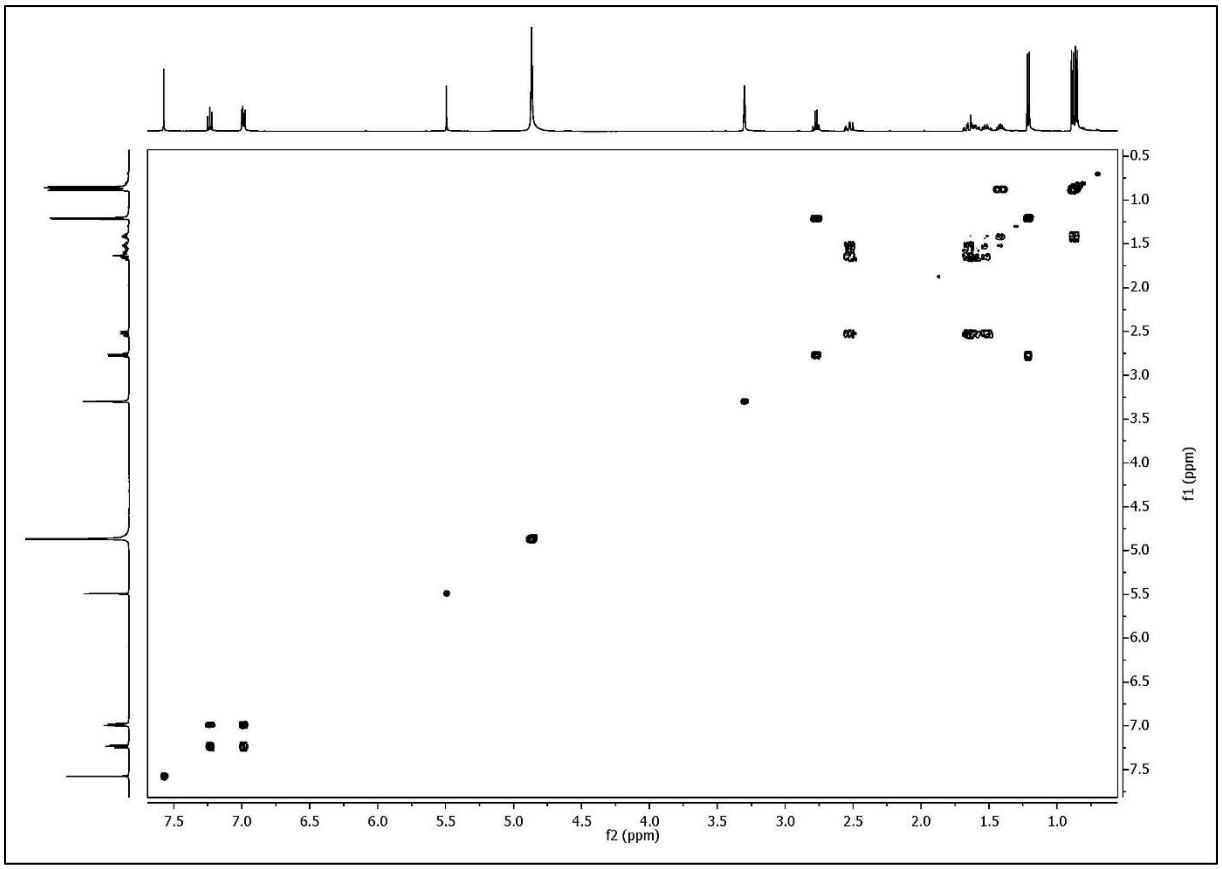

Figure S28. HSQC NMR of rishirilide A (**1**) **(**500MHz, 22°C, CD_3OD)

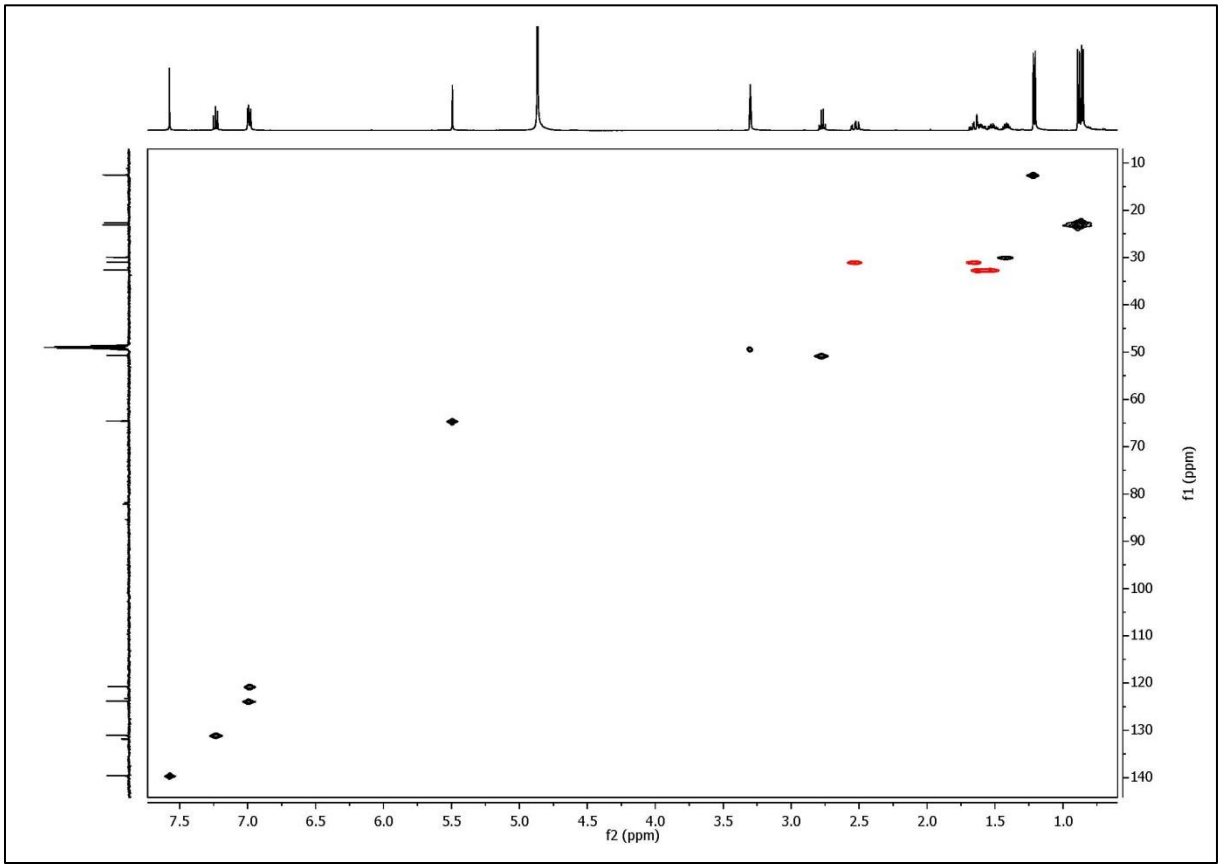

Figure S29. HMBC NMR of rishirilide A (**1**) **(**500MHz, 22°C, CD_3OD)

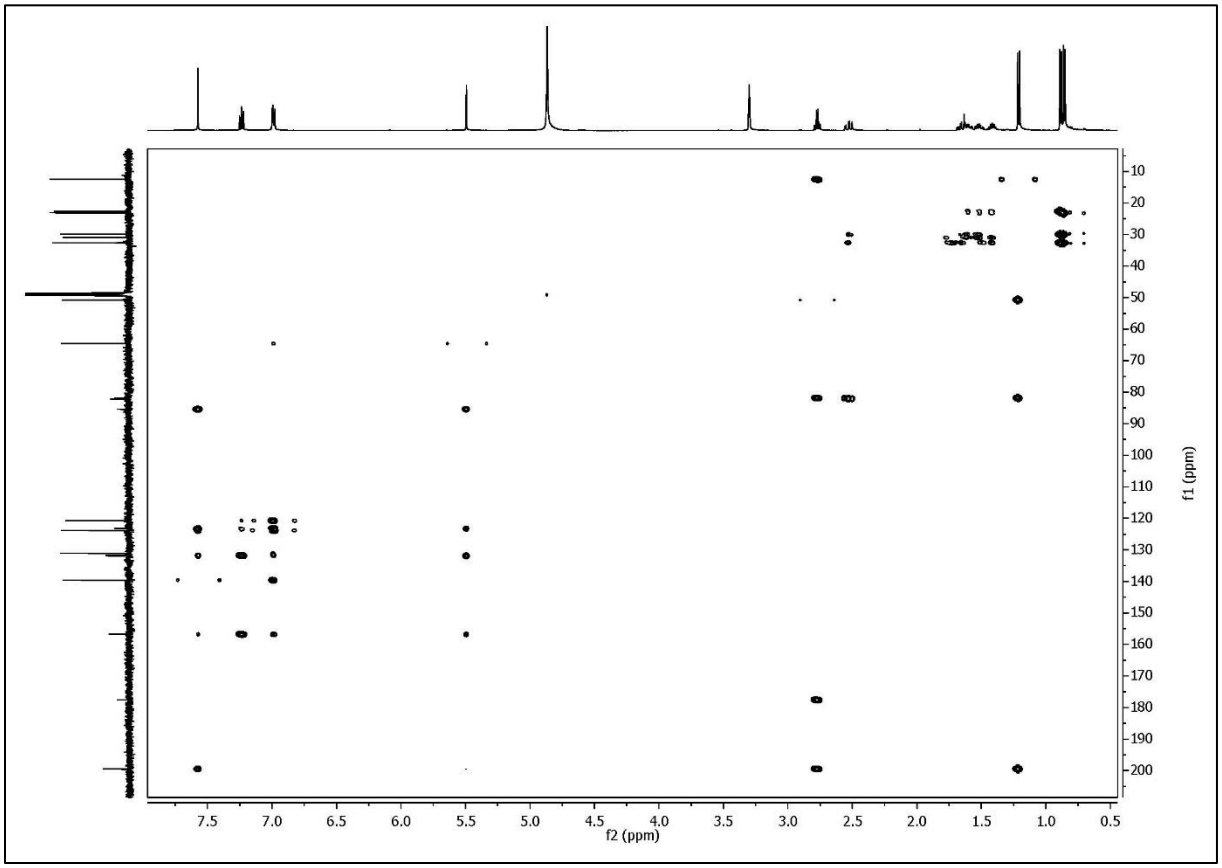

Figure S30. ^{1}H NMR of rishirilide B (**2**) **(**600MHz, 35°C, DMSO-d_6)

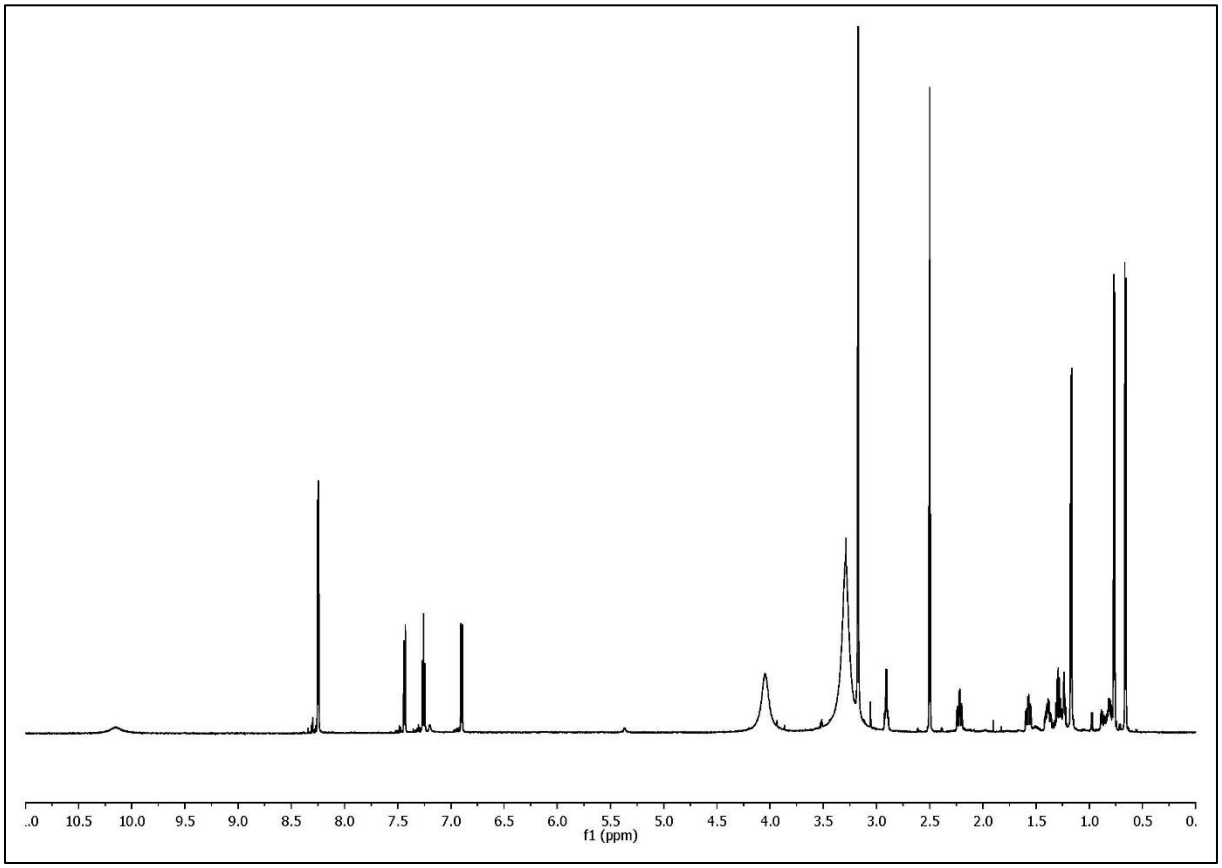

Figure S31. ^{13}C NMR of rishirilide B (**2**) **(**150MHz, 35°C, DMSO-d_6)

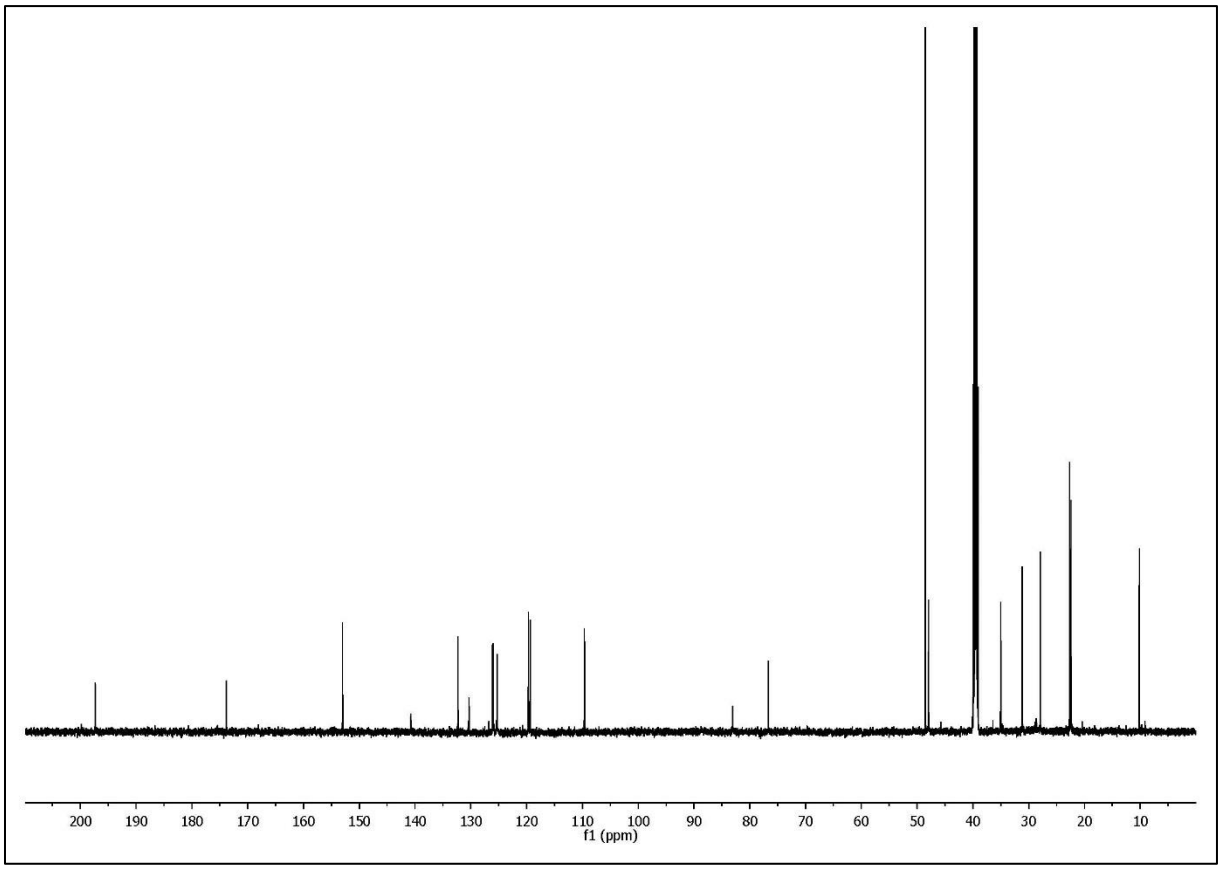

Figure S32. COSY NMR of rishirilide B (**2**) **(**600MHz, 35°C, DMSO-d_6)

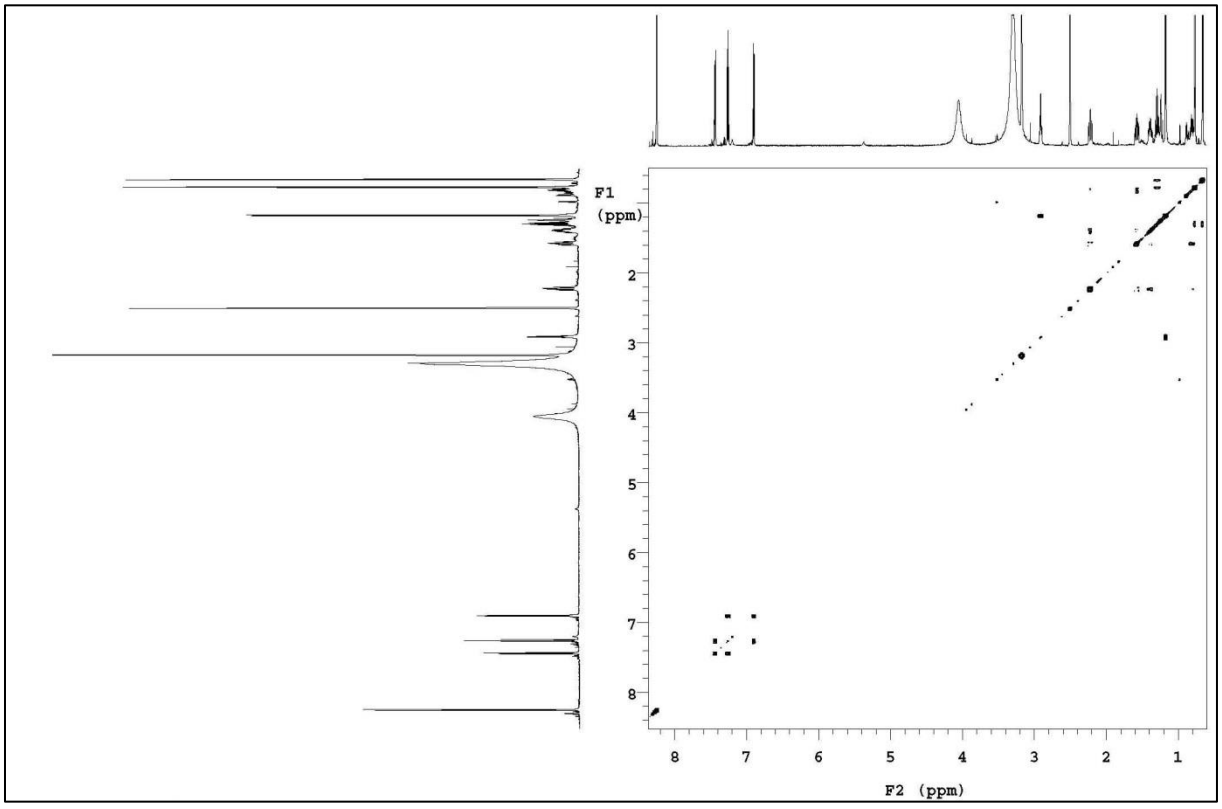

Figure S33. HSQC NMR of rishirilide B (**2**) **(**600MHz, 35°C, DMSO-d_6)

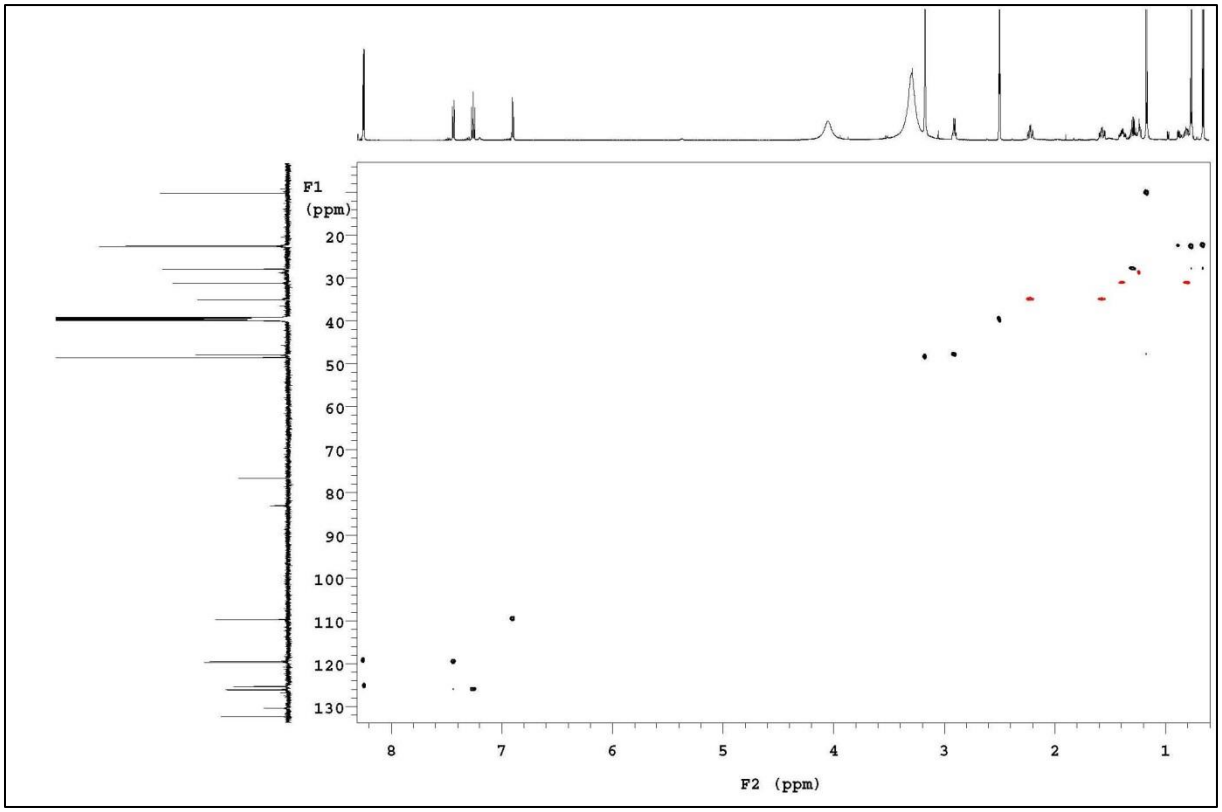

Figure S34. HMBC NMR of rishirilide B (**2**) **(**600MHz, 35°C, DMSO-d_6)

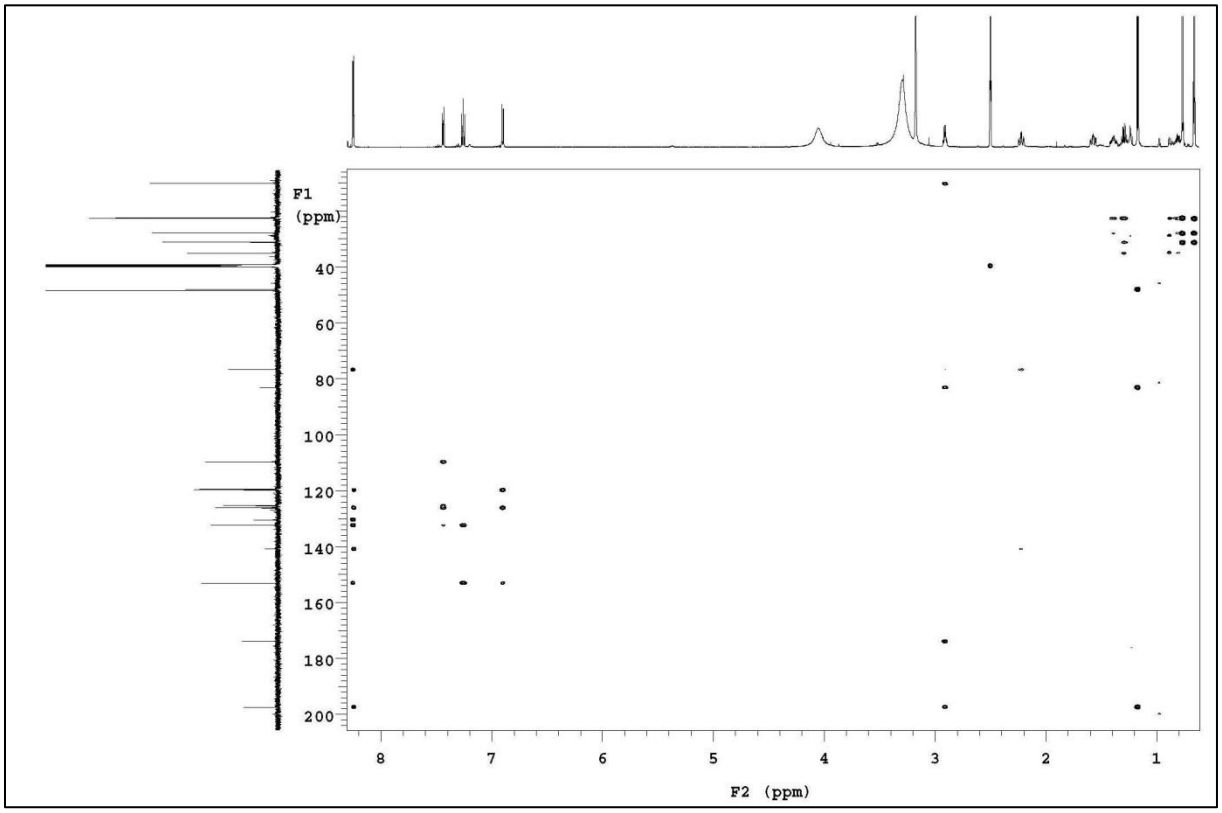

Figure S35. ^{1}H NMR of rishirilide D (**3**) **(**600MHz, 25°C, CD_3OD)

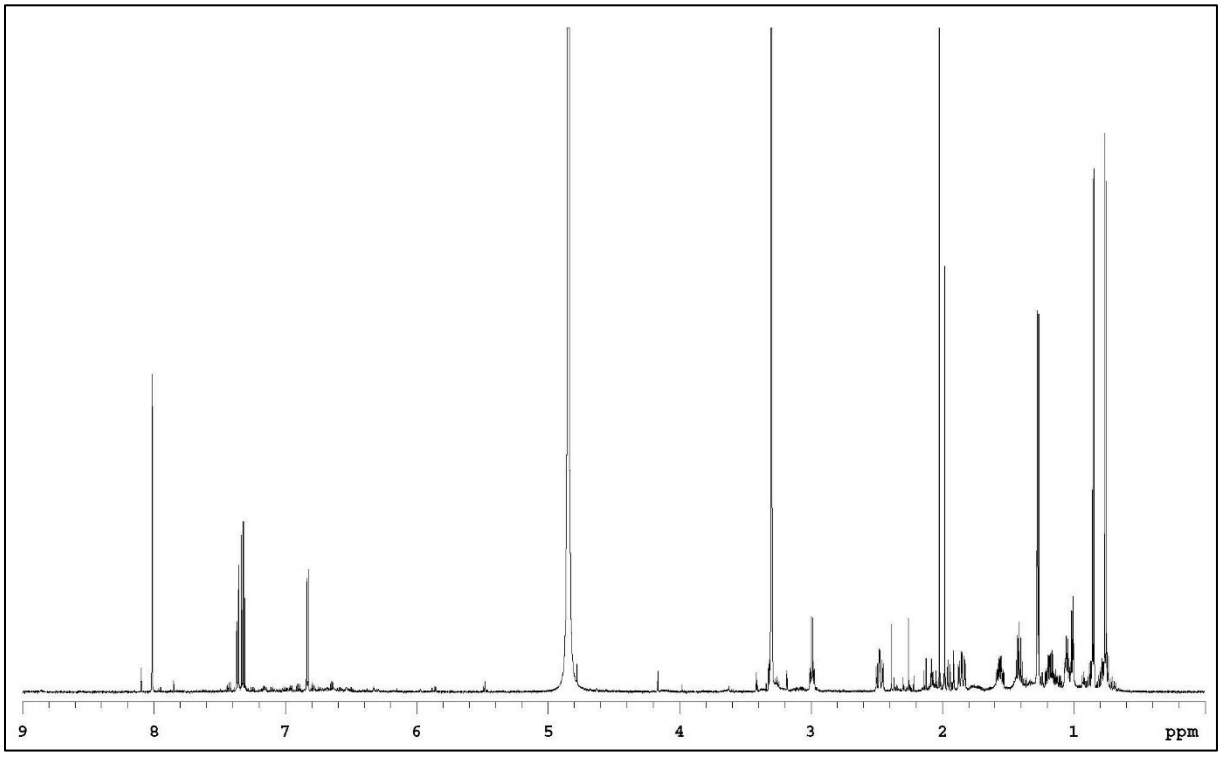

Figure S36. ^{13}C NMR of rishirilide D (**3**) **(**150MHz, 25°C, CD_3OD)

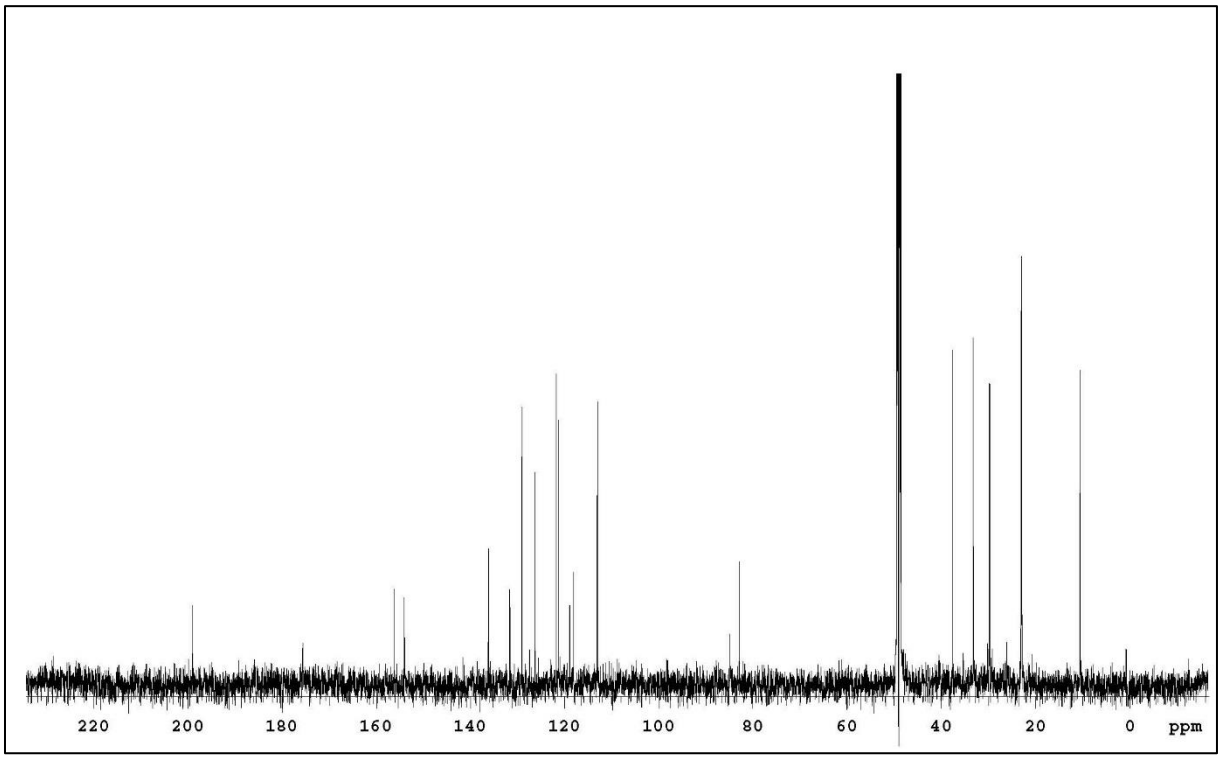

Figure S37. COSY NMR of rishirilide D (**3**) **(**600MHz, 25°C, CD_3OD)

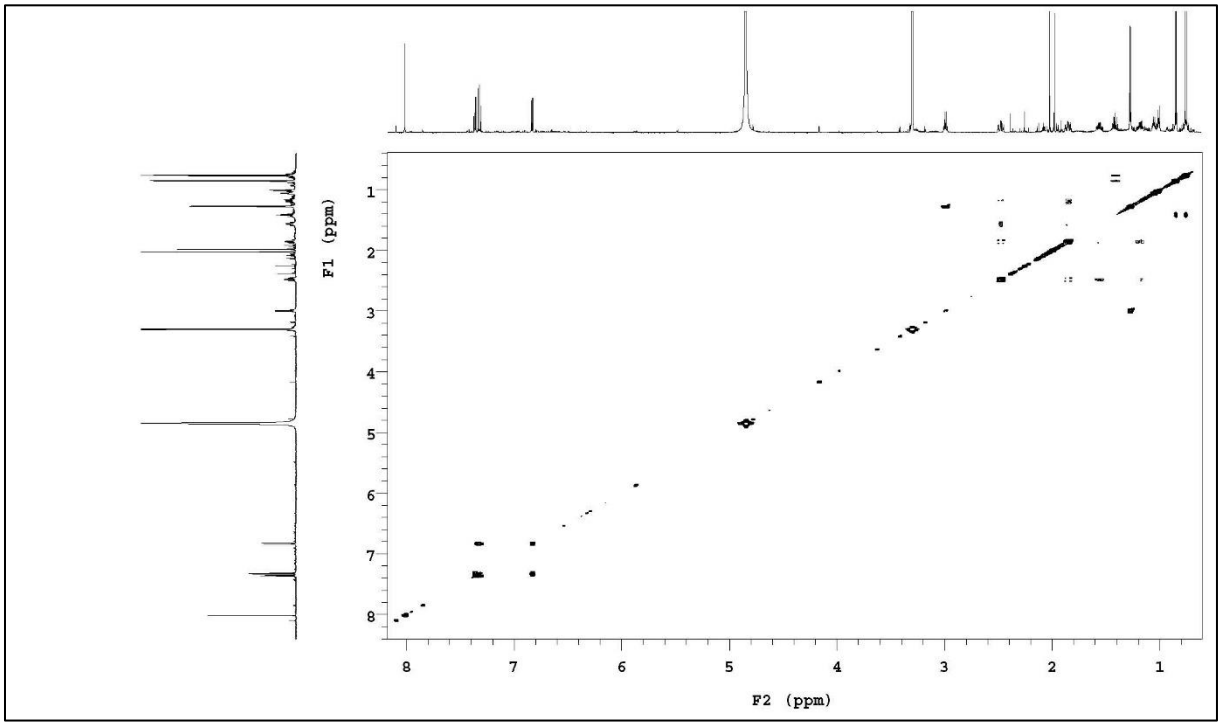

Figure S38. HSQC NMR of rishirilide D (**3**) **(**600MHz, 25°C, CD_3OD)

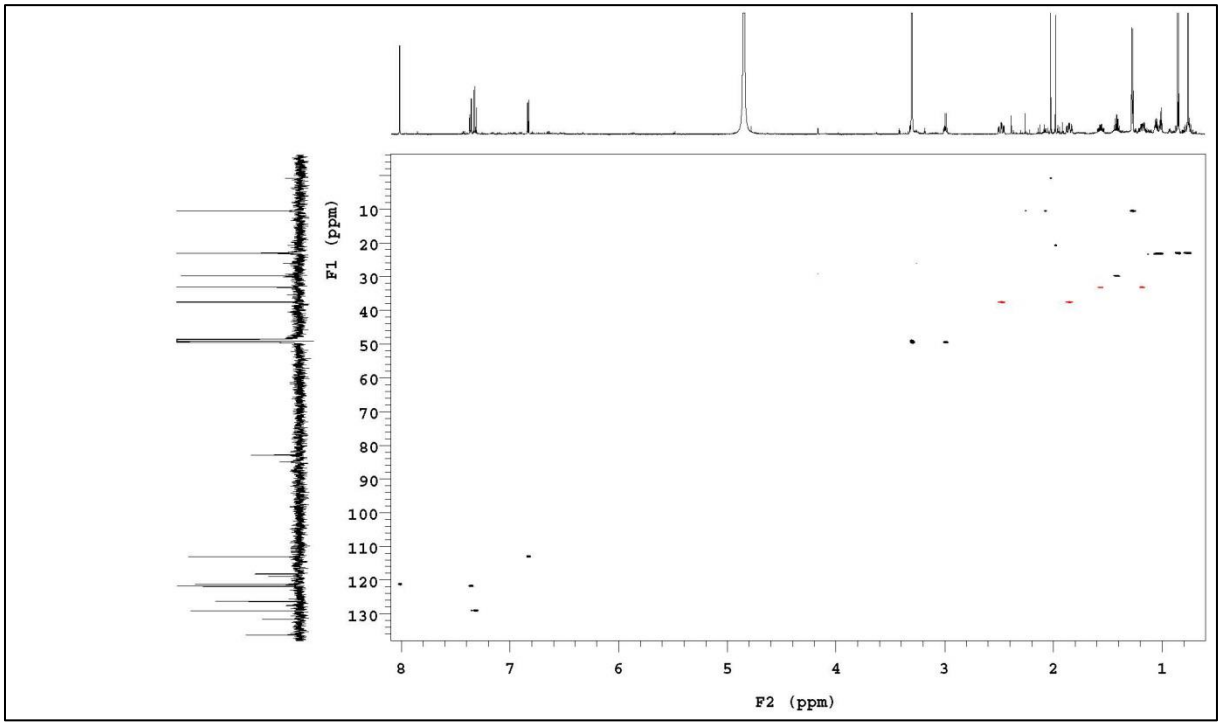

Figure S39. HMBC NMR of rishirilide D (**3**) **(**600MHz, 25°C, CD_3OD)

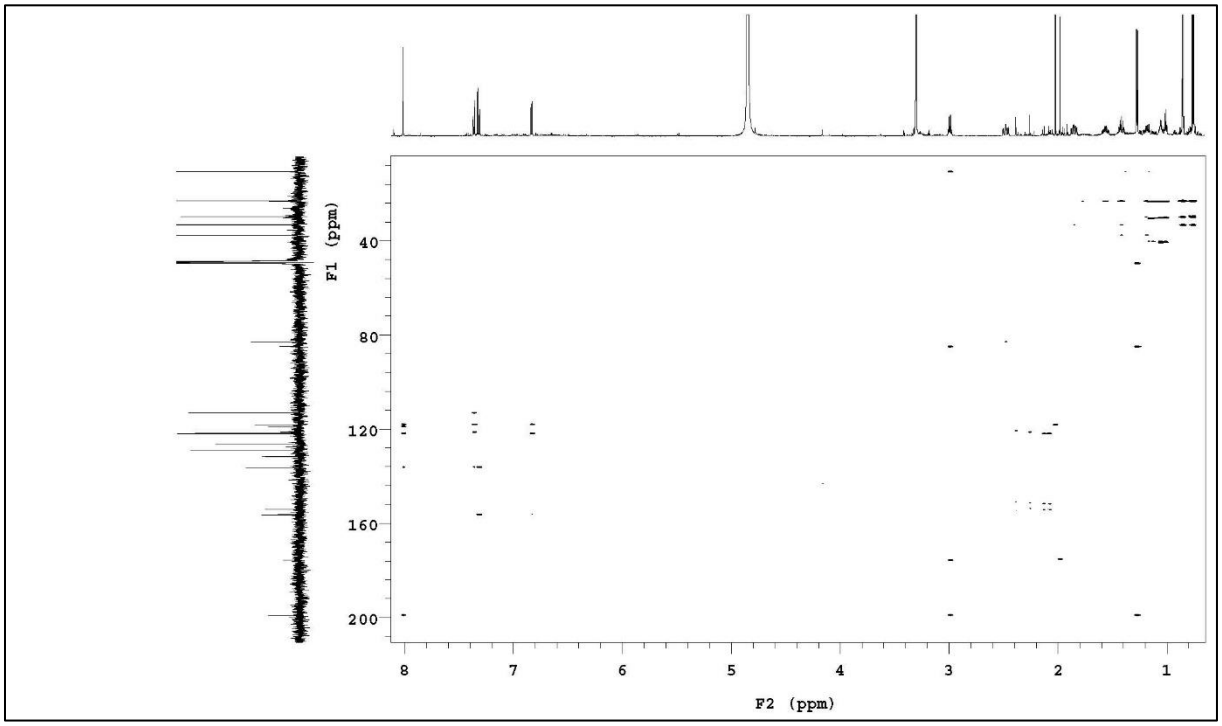

Figure S40. ^{1}H NMR of compound **4 (**600MHz, 25°C, CD_3OD)

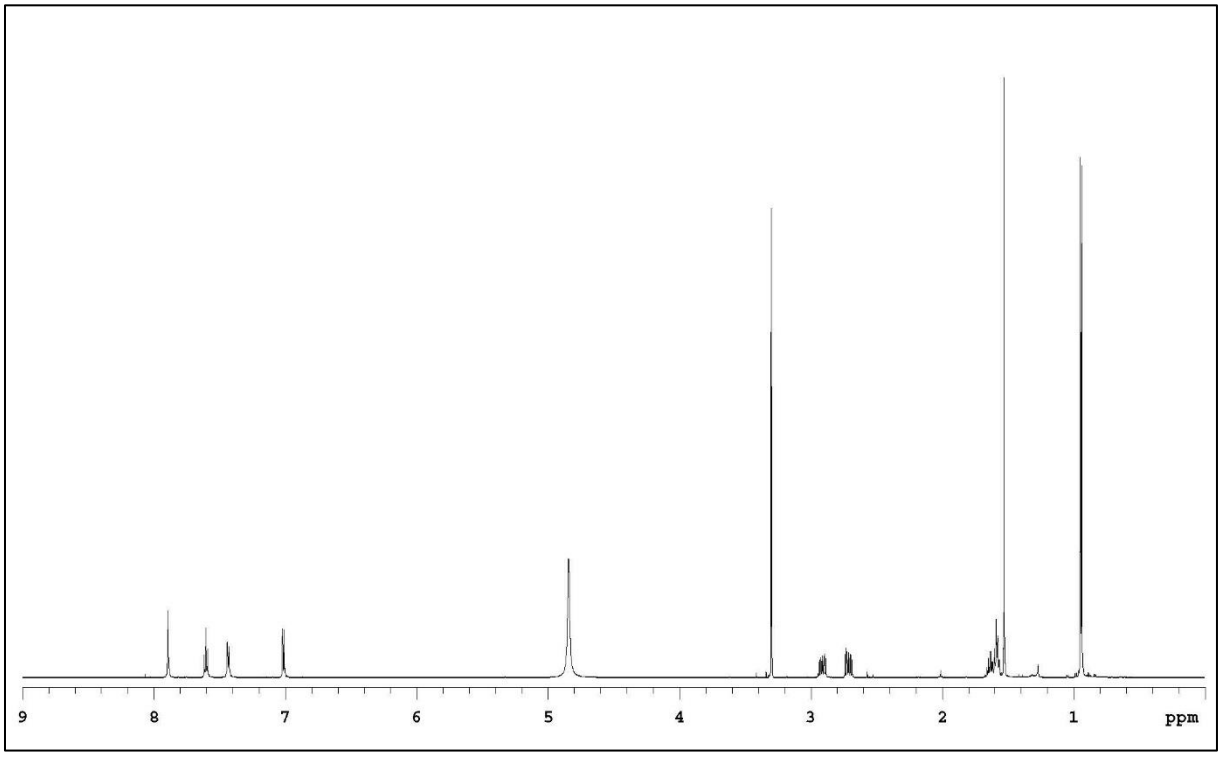

Figure S41. ^{13}C NMR of compound **4 (**150MHz, 25°C, CD_3OD)

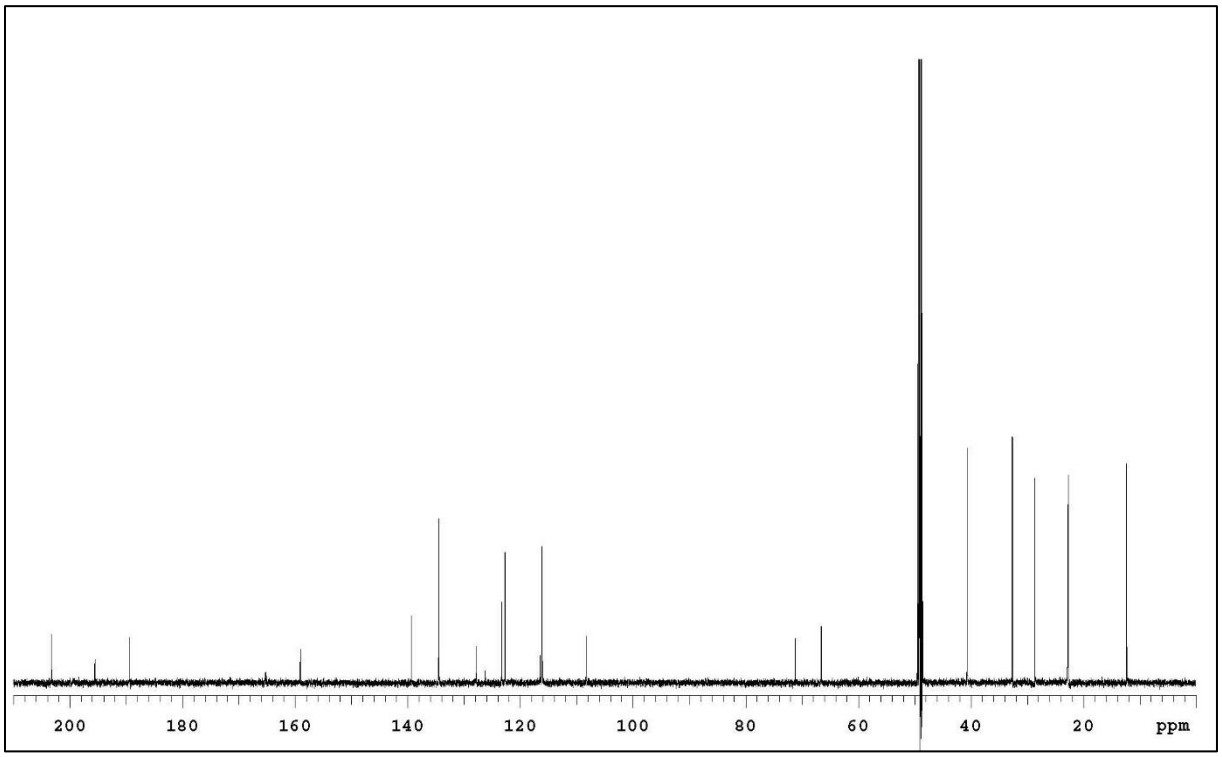

Figure S42. COSY NMR of compound **4 (**600MHz, 25°C, CD_3OD)

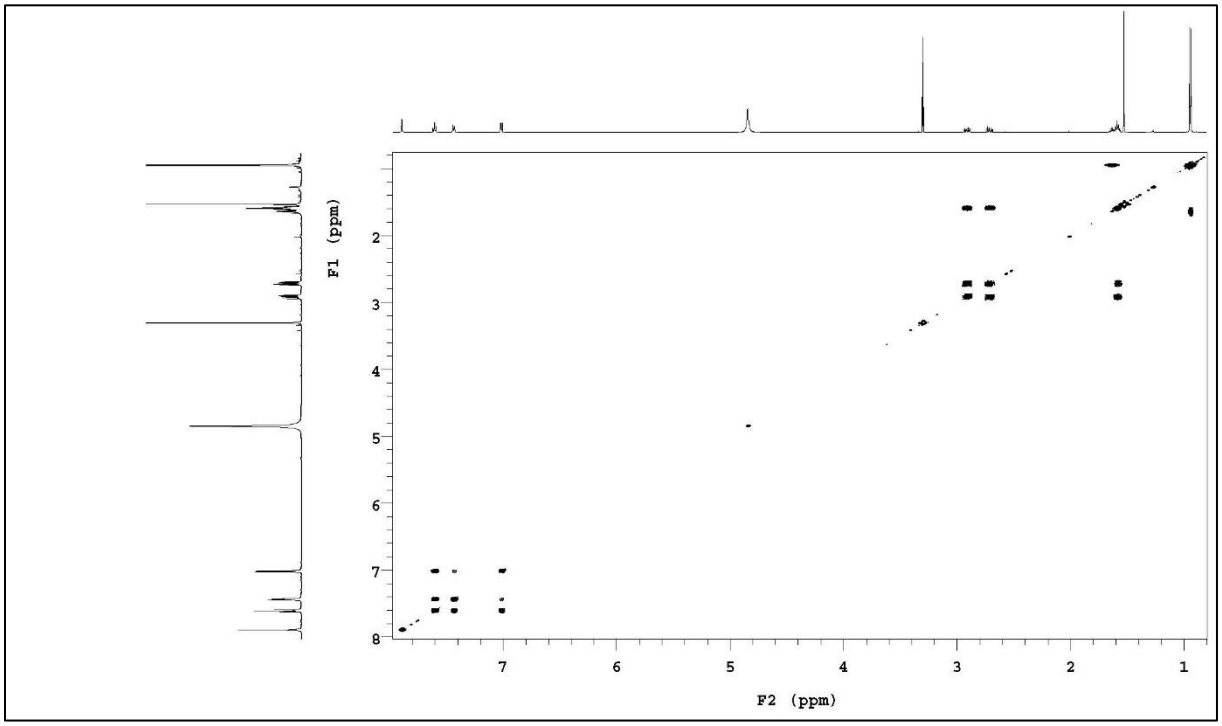

Figure S43. HSQC NMR of compound **4 (**600MHz, 25°C, CD_3OD)

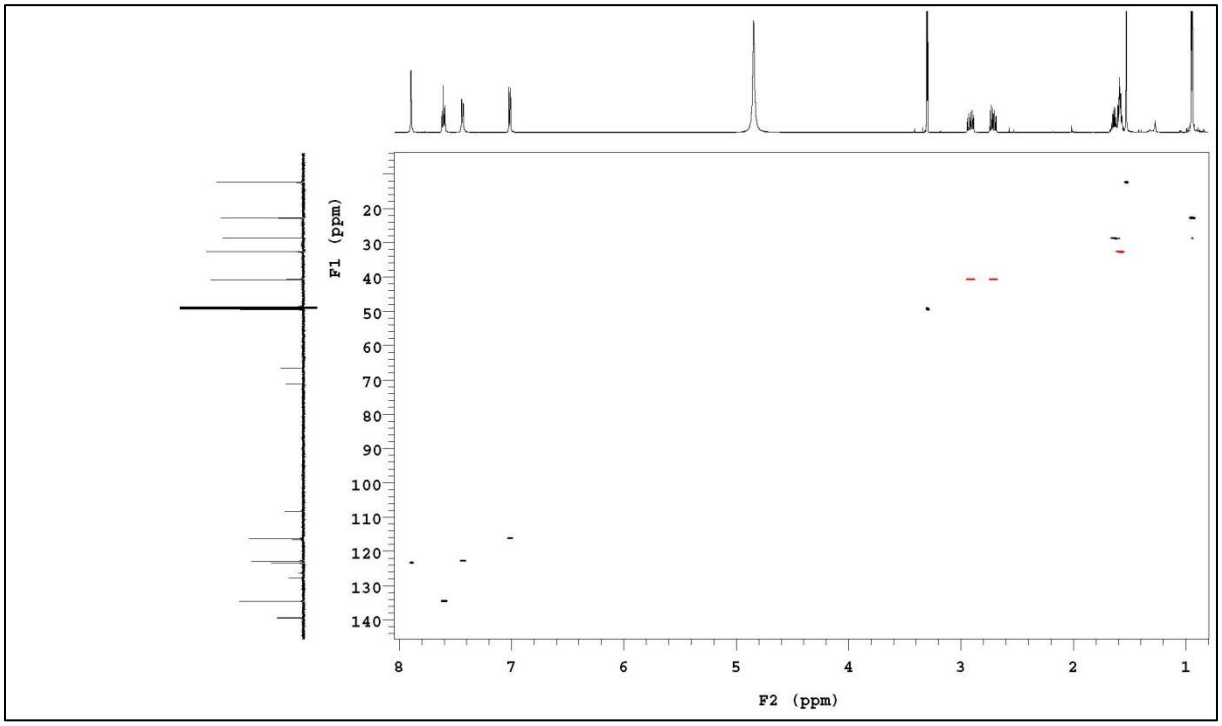

Figure S44. HMBC NMR of compound **4 (**600MHz, 25°C, CD_3OD)

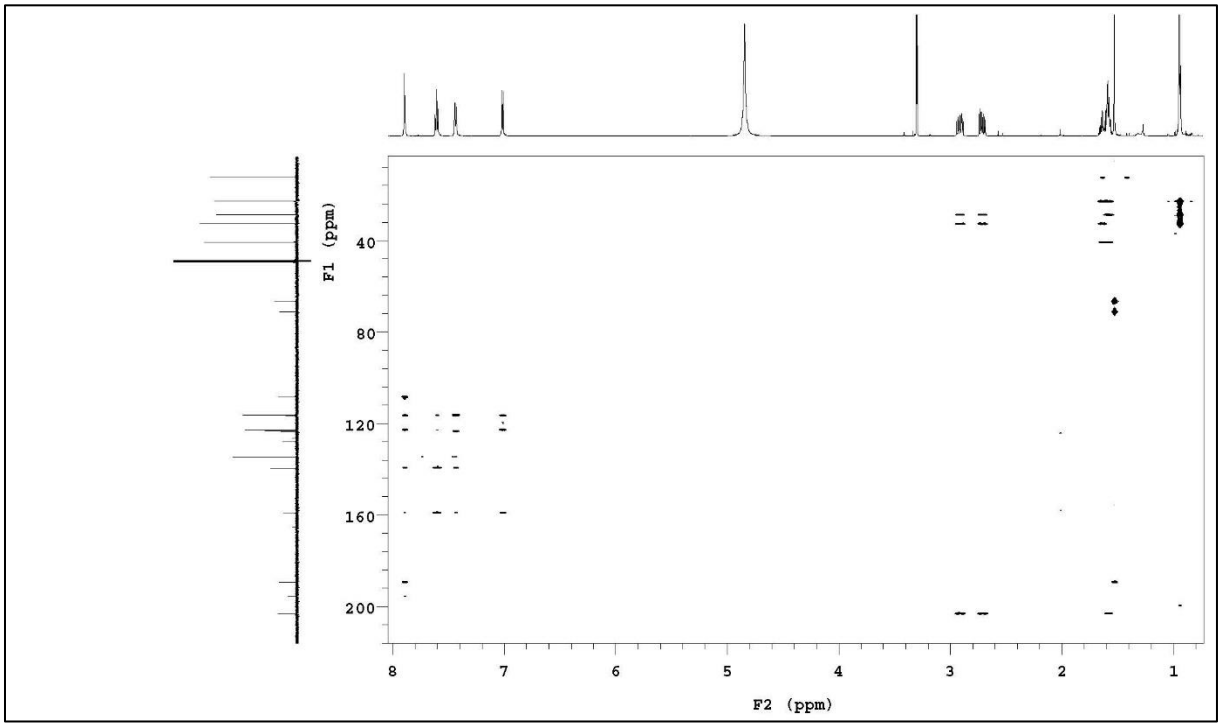

Figure S45. ^{1}H NMR of compound **5 (**600MHz, 25°C, $CDCl_3$)

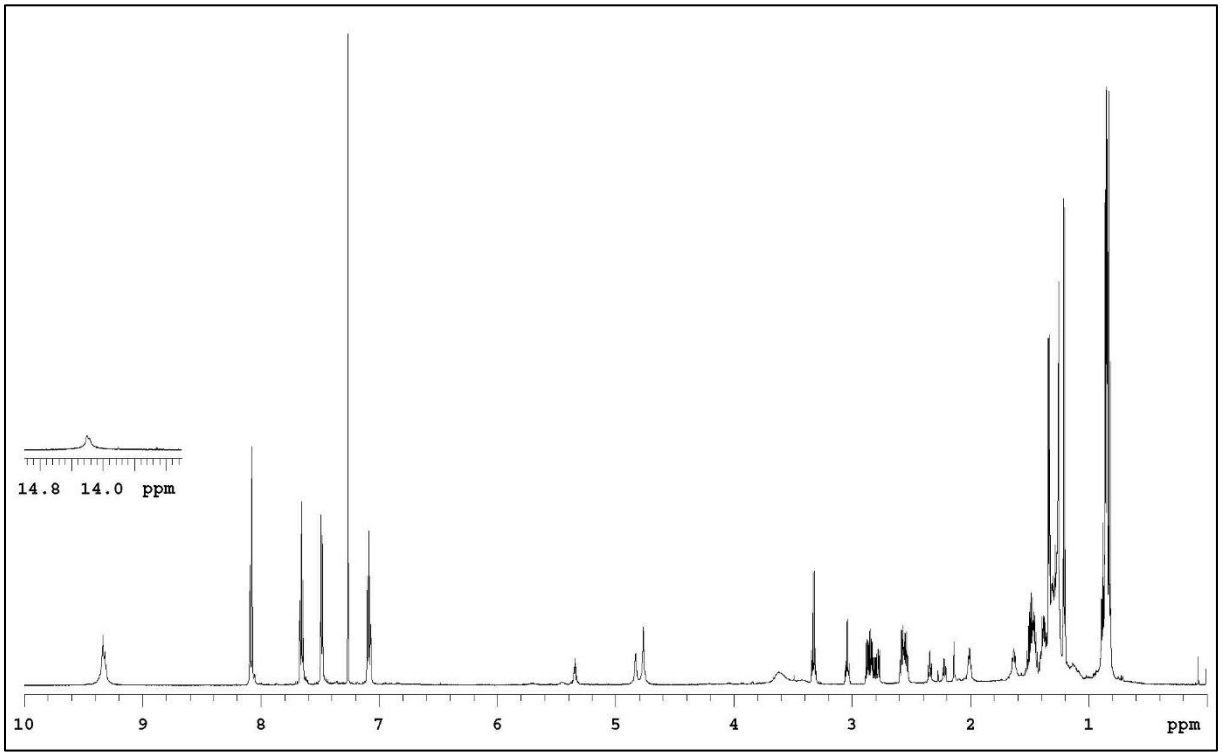

Figure S46. ^{13}C NMR of compound **5 (**150MHz, 25°C, $CDCl_3$)

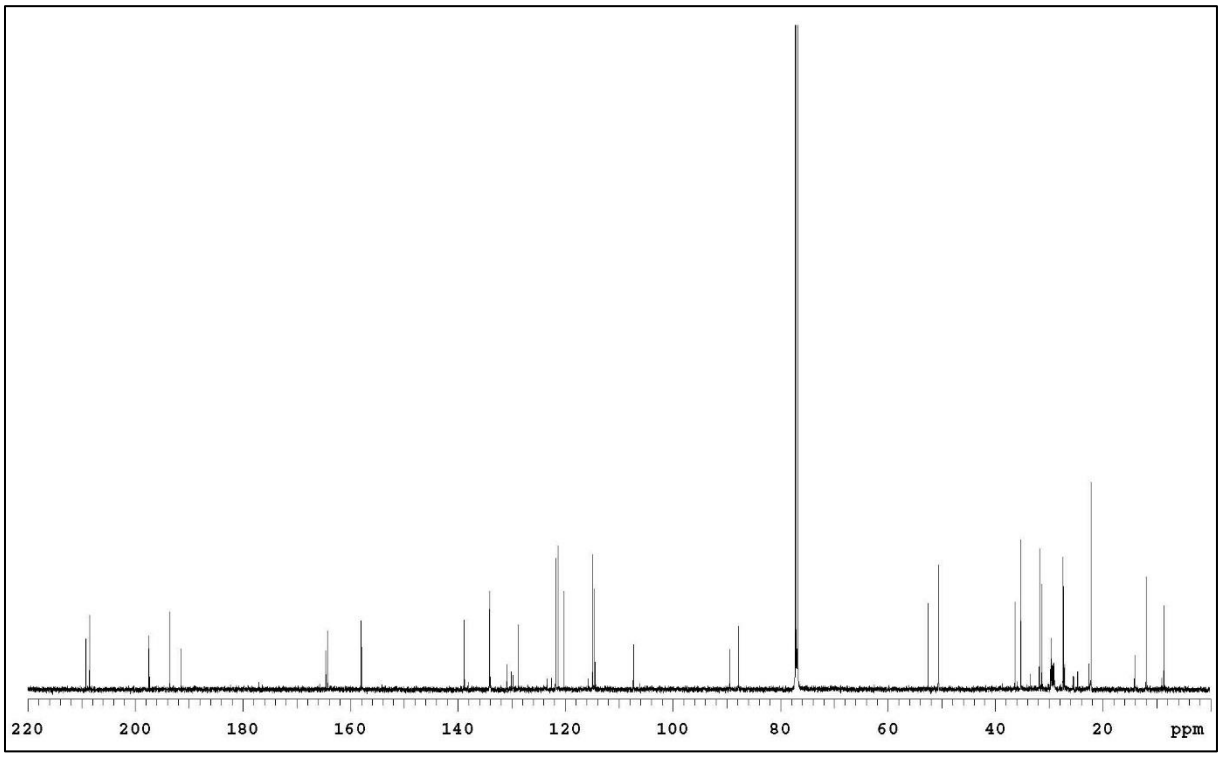

Figure S47. COSY NMR of compound **5 (**600MHz, 25°C, $CDCl_3$)

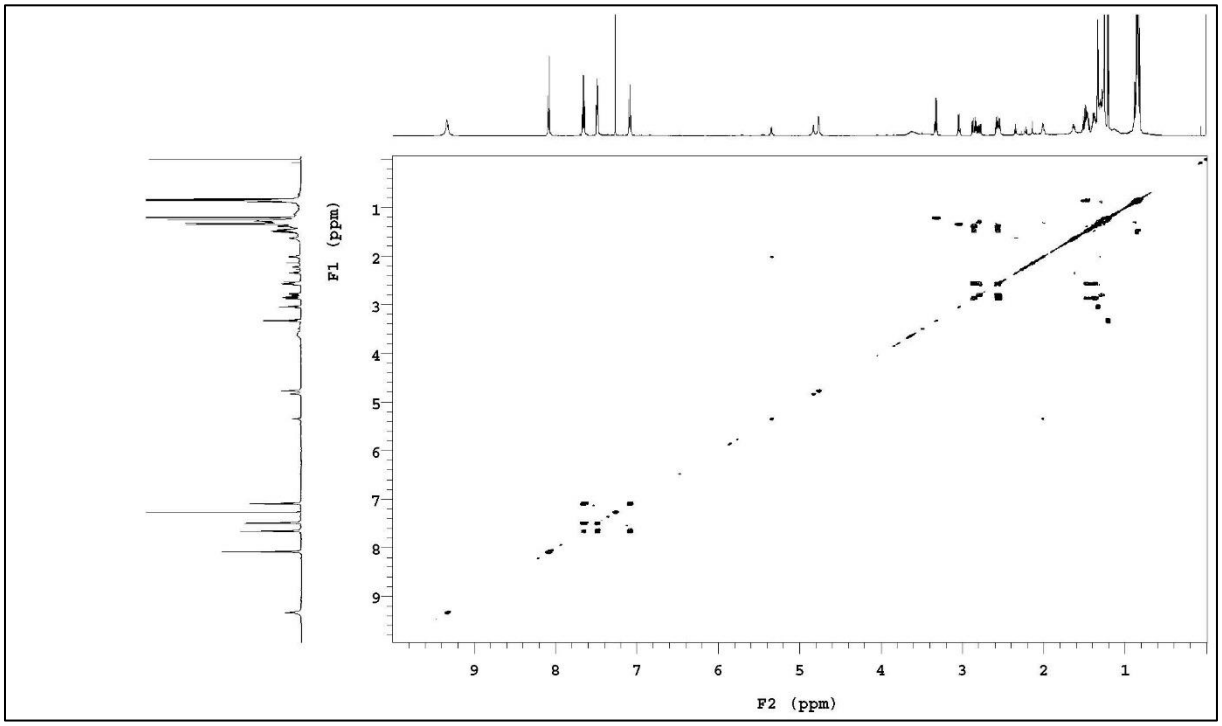

Figure S48. HSQC NMR of compound **5 (**600MHz, 25°C, $CDCl_3$)

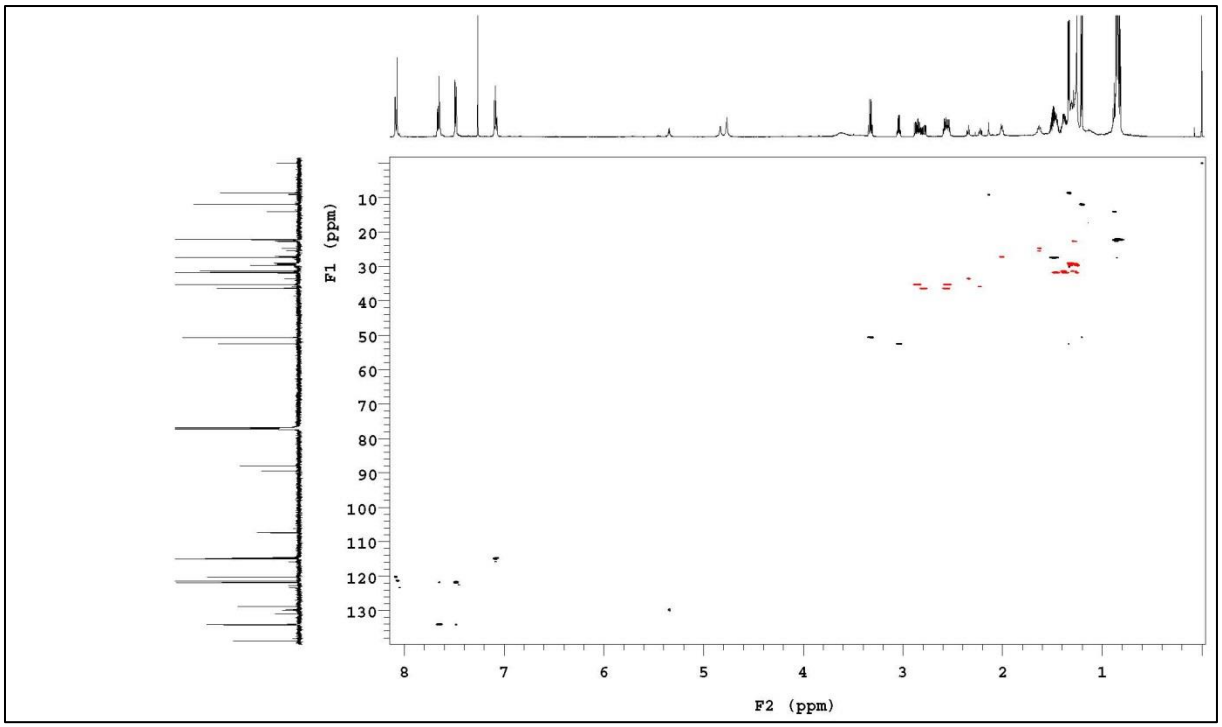

Figure S49. HMBC NMR of compound **5 (**600MHz, 25°C, $CDCl_3$)

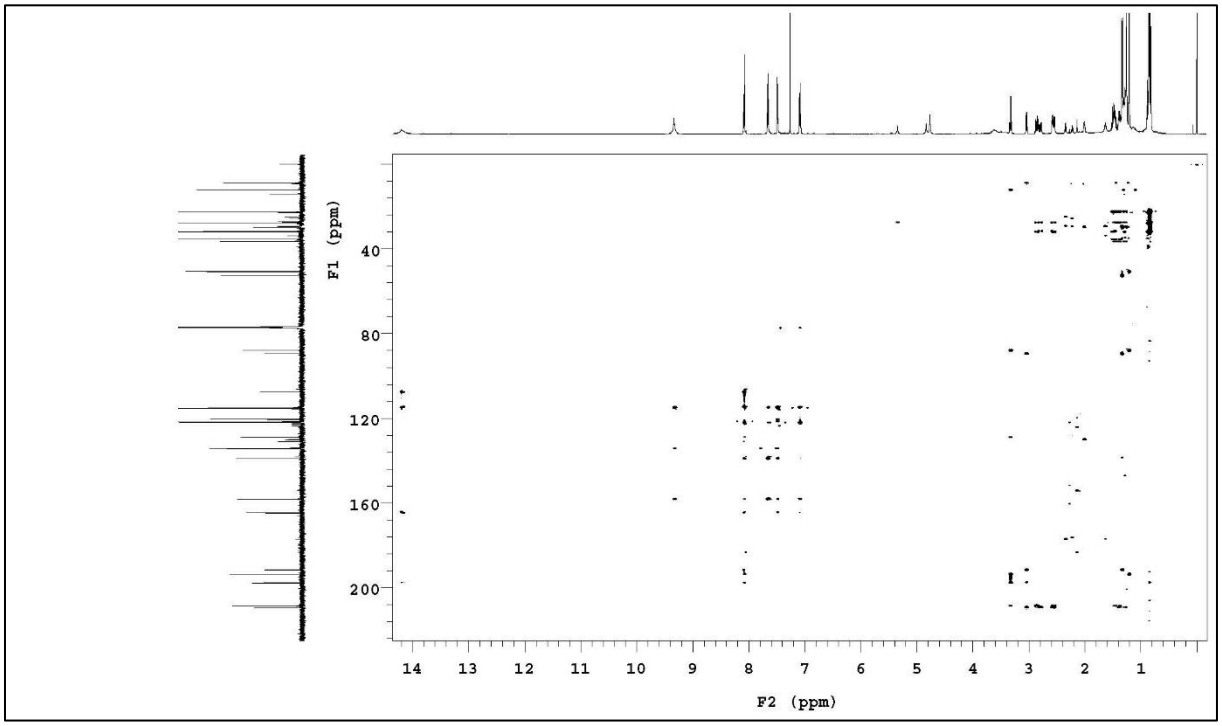

Figure S50. TOCSY NMR of compound **5 (**600MHz, 25°C, $CDCl_3$)

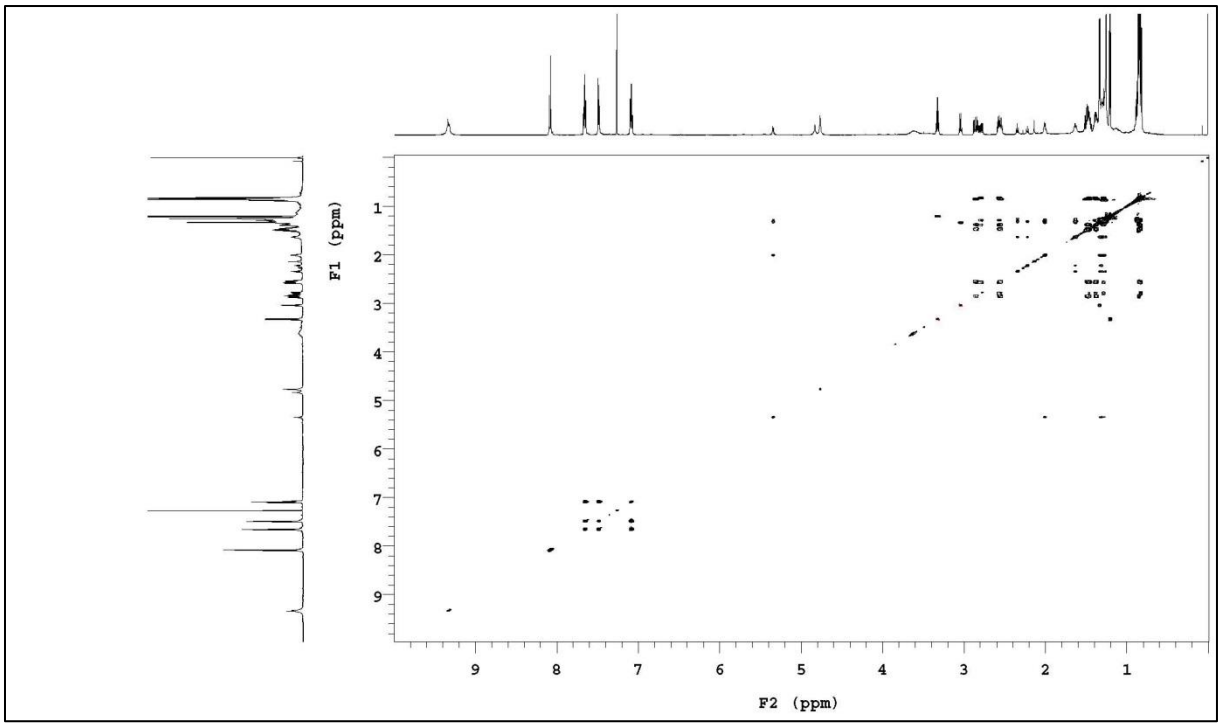

L. References

1. Mazodier, P.; Petter, R.; Thompson, C. Intergeneric conjugation between *Escherichia coli* and *Streptomyces* species. *J Bacteriol.* **1989**, *171*, 3583-3585.
2. Gust, B.; Chandra, G.; Jakimowicz, D.; Yuqing, T.; Bruton, C. J.; Chater, K. F. Lambda red-mediated genetic manipulation of antibiotic-producing *Streptomyces*. *Adv. Appl. Microbiol*. **2004**, *54*, 107-128.
3. Yan, X.; Probst, K.; Linnenbrink, A.; Arnold, M.; Paululat, T.; Zeeck, A.; Bechthold, A. Cloning and heterologous expression of three type II PKS gene clusters from *Streptomyces bottropensis*. *ChemBioChem.* **2012**, *13*, 224-230.
4. Tsypik, O.; Makitrynskyy, R.; Bera, A.; Song, L.; Wohlleben, W.; Fedorenko, V.; Ostash, B. Role of GntR Family Regulatory Gene *SCO1678* in Gluconate Metabolism in *Streptomyces coelicolor* M145. *BioMed Res. Internat.* **2017**, 9529501, p.9.
5. Fedoryshyn, M.; Welle, E.; Bechthold, A.; Luzhetskyy, A. Functional expression of the Cre recombinase in actinomycetes. *Appl. Microbiol. Biotechnol.* **2008**, *78*, 1065–1070.
6. Zhang, C.; Sun, C.; Huang, H.; Gui, C.; Wang, L.; Li, Q.; Ju, J. Biosynthetic Baeyer-Villiger Chemistry Enables Access to Two Anthracene Scaffolds from a Single Gene Cluster in Deep-Sea-Derived *Streptomyces olivaceus* SCSIO T05. *J. Nat. Prod.* **2018**, *81*, 1570–1577.